PROJECT REPORT

On

"PREPARATION AND CHARACTERIZATION OF ECO-FRIENDLY CHITOSAN-STARCH MONTMORILLONITE NANOCOMPOSITE BY IN-SITU INTERCALATION AND ITS APPLICATION IN REACTIVE DYE REMOVAL"

Submitted by

SEETHALAKSHMI C. S.
(AM23CHE013)

In partial fulfillment for the award of the Postgraduate Degree in Chemistry

**DEPARTMENT OF CHEMISTRY
AND
CENTRE FOR RESEARCH**

**ST. TERESA'S COLLEGE (AUTONOMOUS)
ERNAKULAM**

2024-2025

DEPARTMENT OF CHEMISTRY
AND
CENTRE FOR RESEARCH
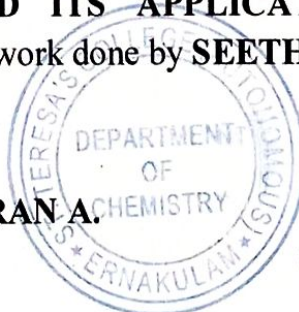
ST. TERESA'S COLLEGE (AUTONOMOUS)

ERNAKULAM

M.Sc. CHEMISTRY PROJECT REPORT

Name	: SEETHALAKSHMI C. S.
Register Number	: AM23CHE013
Year of Work	: 2024-2025

This is to certify that the project **"PREPARATION AND CHARACTERIZATION OF ECO-FRIENDLY CHITOSAN-STARCH MONTMORILLONITE NANOCOMPOSITE BY IN-SITU INTERCALATION AND ITS APPLICATION IN REACTIVE DYE REMOVAL"** is the work done by **SEETHALAKSHMI C. S.**

DR. SARITHA CHANDRAN A.
Head of the Department

DR. ANNU RAJU
Staff-member in charge

Submitted to the Examination of Master's degree in Chemistry

Date: 29/4/2025

Examiners: 1. Dr. DEEPA. C.S

2. Dr. Rony Rajan Paul

ST.TERESA'S COLLEGE (AUTONOMOUS)
ERNAKULAM

Certificate of Plagiarism Check for Dissertation

Author Name	JENI MOL P. M., SEETHALAKSHMI C. S.
Course of Study	M.Sc. Chemistry
Name of Guide	Dr. Annu Raju
Department	Chemistry & Centre For Research
Acceptable Maximum Limit	20
Submitted By	library@teresas.ac.in
Paper Title	"PREPARATION AND CHARACTERIZATION OF ECO-FRIENDLY CHITOSAN-STARCH MONTMORILLONITE NANOCOMPOSITE BY IN-SITU INTERCALATION AND ITS APPLICATION IN REACTIVE DYE REMOVAL"
Similarity	6% AI - 15%
Paper ID	3380829
Total Pages	112
Submission Date	2025-03-06 12:41:41

Signature of Student

Signature of Guide

Checked By
College Librarian

CERTIFICATE

This is to certify that the project work titled **"PREPARATION AND CHARACTERIZATION OF ECO-FRIENDLY CHITOSAN-STARCH MONTMORILLONITE NANOCOMPOSITE BY IN-SITU INTERCALATION AND ITS APPLICATION IN REACTIVE DYE REMOVAL"** is the work done by **SEETHALAKSHMI C. S.** under the guidance of **DR. ANNU RAJU**, Assistant Professor, Department of Chemistry and Centre for Research, St. Teresa's College, Ernakulam in partial fulfilment of the award of the Degree of Master of Science in Chemistry at St. Teresa's College, Ernakulam affiliated to Mahatma Gandhi University, Kottayam.

DR. ANNU RAJU
Project Guide

DR. SARITHA CHANDRAN A.
Head of the Department

CERTIFICATE

This is to certify that the project work entitled **"PREPARATION AND CHARACTERIZATION OF ECO-FRIENDLY CHITOSAN-STARCH MONTMORILLONITE NANOCOMPOSITE BY IN-SITU INTERCALATION AND ITS APPLICATION IN REACTIVE DYE REMOVAL"** is the work done by **SEETHALAKSHMI C. S.** under my guidance in the partial fulfilment of the award of the Degree of Master of Science in Chemistry at St. Teresa's College (Autonomous), Ernakulam affiliated to Mahatma Gandhi University, Kottayam.

DR. ANNU RAJU
Project Guide

DECLARATION

I hereby declare that the project work entitled **"PREPARATION AND CHARACTERIZATION OF ECO-FRIENDLY CHITOSAN-STARCH MONTMORILLONITE NANOCOMPOSITE BY IN-SITU INTERCALATION AND ITS APPLICATION IN REACTIVE DYE REMOVAL"** submitted to Department of Chemistry and Centre for Research, St. Teresa's College (Autonomous) affiliated to Mahatma Gandhi University, Kottayam, Kerala is a record of an original work done by me under the guidance of **DR. ANNU RAJU**, Assistant Professor, Department of Chemistry and Centre for Research, St. Teresa's College (Autonomous), Ernakulam. This project work is submitted in the partial fulfillment of the requirements for the award of the Degree of Master of Science in Chemistry.

SEETHALAKSHMI C. S.

Acknowledgements

First of all, I would like to thank **Almighty God** for the successful completion of this project.

I express my heartfelt thanks to my project supervisor **Dr. Annu Raju**, my guide, Assistant Professor, St Teresa's College for her guidance, suggestions and encouragement for the successful completion of this project.

I would like to express my deep sense of gratitude to **Dr. Saritha Chandran A.**, Head of the Department of Chemistry and Centre for Research, St Teresa's College for her constant encouragement and motivations.

I take this opportunity to express my sincere thanks to **Dr. Alphonsa Vijaya Joseph**, Principal, St. Teresa's College, Ernakulam and Manager **Rev. Sr. Nilima**, Directors **Rev. Sr. Francis Ann** and **Rev. Sr. Tessa CSST**, St. Teresa's College, Ernakulam, for being the pillars of support and providing good infrastructure for the study and development of students.

I express my heartfelt thanks to all Teachers of the chemistry department, for their wholehearted help and advices during the academic year, I also remember fondly the valuable support of the non-teaching staff of the department during chemistry lab hours and the project hours.

I heartily thank **STIC (CUSAT)** for providing all the spectroscopic assistance needed for the characterization of the samples within the time limit.

I thank **Department of Zoology** and **Teresian Instrumentation and Consultancy Centre (TICC)** St Teresa's College, for their support and guidance for my project.

Last, but not least, I am grateful to my loving families and friends for the care, support, and concern they provide to follow my passion.

SEETHALAKSHMI C.S.

Contents

Chapter 1

Introduction

1. IMPACT OF DYES IN WATER POLLUTION

Rising concerns about environmental pollution from industrial dyes highlight the need for sustainable and efficient adsorbents. Nanocomposites have become important in wastewater treatment due to unique properties that distinguish them from others. Breakthroughs in nanotechnology have revolutionized the concept of wastewater treatment. Nanocomposites with remarkable adsorption capacities are going to change the game. It is a promising approach for the reasons of its large surface area, tunable properties, and molecular-level interaction with pollutants.

Water pollution, specifically by the textile industry, seriously poses health threats to the environment. The cause is reactive dyes. It is toxic and very resistant to biodegradation. This water pollution ranks as one of the biggest threats to ecosystems, public health, and sustainable development. Water sources are getting increasingly polluted with chemicals, heavy metals, and dyes owing to the consequences of the rise of industry and urbanization. Reactive dyes used in the textile industry are very problematic due to their high toxicity, corrosion resistance, and survival in aquatic environments.

Nowadays, removing harmful contaminants from wastewater has attracted significant attention due to their severe adverse effects on both the environment and human health. Rapid industrialization and urbanization in

1

developing countries in the last few decades have contributed to environmental decline. A vast amount of untreated or inadequately treated wastewater is released into the environment. This poses a significant barrier to the sustainability of the ecosystem. Therefore, there is a need to embrace state-of-the-art and relatively cost-effective wastewater treatment technology. Among other techniques, nanomaterials science has recently gained great scientific attention. Examples of nano-adsorbents include carbon nanotubes, titanium oxide, manganese oxide, activated carbon (AC), magnesium oxide, graphene, ferric oxides, and zinc oxide for pollutant elimination (1). The major environmental concern is water contamination, which is a result of the presence of heavy metal ions. Metals such as Ni, Co, Zn, Pt, Pd, Ag, Cu, Cd, Pb, and Hg are introduced to the environment either from natural processes or anthropogenic activities. They are mostly released as a result of weathering and human sources like chemical manufacture, electroplating, battery production, pesticide, and fertilizer industries are additional contributors to their presence. With low concentrations in the environment, the metal ions are capable of entering the food chain and subsequently being inhaled by humans, leading to the accumulation of metals in the human system and causing severe health issues (2). The ring-opening polymerization of phenyl amino methyl trimethoxysilane (PAMTMS) and pyromellitic acid dianhydride (PMDA), followed by a sol-gel procedure, produced several zwitterionic hybrid polymers. These polymers can adsorb Cu^{2+} and Pb^{2+} (3).

The effectiveness of the regeneration as well as the adsorption efficiency of the different adsorbents is a very important factor in the treatment of the industrial dyes and the control of water pollution. Different methods and substances are applied to remove organic pollutants from water, and one of them is the method of adsorption which is the most effective.

2

The cost-effective and eco-friendly clay-supported adsorbents are highly used due to their simple design and environmental soundness. While activated carbon is very efficient in the removal of dyes, that is because natural adsorbents like coal are highly efficient. Nevertheless, the application of this material is limited by high regeneration costs. Clays and modified clay-based adsorbents are very suitable to be used as more efficient and economical replacements for removing organic pollutants (4).

Starch stands out as one of the leading biopolymers worldwide and is very well-renowned among natural polymers for its unique physical and chemical properties. Its promise as a renewable replacement for petroleum-derived products is the reason behind its gaining attention. Yet on the one hand, starch is considered to be non-ideal for certain applications alone. Starch-clay nanocomposites are an innovative idea that is both environmentally friendly and holds better properties. These clay nanofillers are now very popular in the production of biodegradable starch film and they can improve the properties that are usually presented with traditional fillers. In addition to its benefits, starch-based polymers are tough materials that are sensitive to both mechanical properties and environmental factors like pH, humidity, and temperature. The addition of clay to starch can help to minimize these constraints, thus leading to a high stability level and best performance (5).

Chitosan, a linear polymer that is created by the deacetylation of chitin, is naturally found in the exoskeletons of crustaceans, insect cuticles, and the cell walls of certain fungi. The peculiar nature of the substance is granting fresh bursts of ideas across the academic and industrial fields and even the development of novel compounds and formulations out of chitosan. Chitosan is a chitin-derived biopolymer with high molecular weight,

biocompatibility, non-toxicity, cationic character, and biodegradability. Its extraordinary features have made it commercially viable in the field of pharmaceutical and biomedical sectors (6), (7).

Na^+-montmorillonite and water-soluble polymeric chitosan, underwent an ion exchange reaction to create chitosan–montmorillonite nanocomposites. Strong electrostatic forces between cationic chitosan molecules and anionic silicate layers significantly increased the thermal stability of chitosan in the interlayer space (8). To create the starch-montmorillonite polyaniline (St-MMT/PANI) nanocomposite, aniline was chemically oxidatively polymerized when starch-montmorillonite nanocomposite dispersion was present. In a very little period of contact, this nanocomposite eliminates the dye. Both the adsorption and electrostatic attraction between the dye molecules and the nanocomposite served as the foundation for the removal mechanism (9).

1.1 CLAY

A naturally occurring substance that is widely available on Earth is clay. Fine-grained hydrous aluminum silicate makes up the majority of its composition. Clay minerals are a promising material for the twenty-first century because they are abundant, affordable, and environmentally benign, regardless of whether they are in their fully pure or modified form.

An independent, multifaceted new field called "argillology " or "clay Science is dedicated to studying the characteristics of clays and clay minerals (10). Clays are composed of microcrystalline particles of a small group of minerals, referred to as clay minerals (11).

Different types of Clay
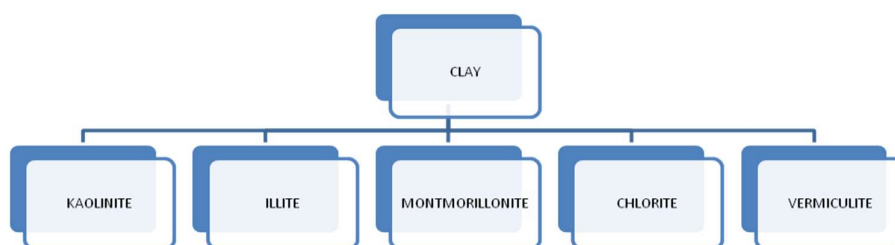
Fig. 1.1 Different types of clay

In a polymer state, the clays themselves can be dispersed at the nanoscale, thereby generating nanocomposites that might enhance the material's thermo-mechanical properties. Clay is an intriguing subject for study because of its many characteristics, forms, and uses (12). At the end of 1985, Toyota Central Research Laboratory coined the name "nanocomposites" while creating automobile cover belts using nylon - montmorillonite (MMT) clay-based nanocomposites. Subsequently, much research was carried out globally in the field of polymer nanocomposites (13). Various kinds of polymer nanocomposites have found uses throughout construction, automotive, packaging, flame retardant, protective film, and other fields. It has been shown that adding clay can significantly improve the characteristics of polymers and cause new unexpected traits to emerge. This is because adding nanofillers to polymers allows for exact tuning of their properties. Nanoparticles are dispersed throughout a polymer matrix in multiphase systems; in the case of polymer nanocomposites, this matrix contains at least one nanoscale dimension (14).

Fig.1.2 Pictures of different clays

Clay belongs to the class of natural or manmade minerals known as layered silicates which are composed of regular stacks of aluminosilicate layers with a high aspect ratio and large surface area. Layered silicates are commonly available and reasonably priced. The most commonly used layered silicates at the moment for creating polymer nanocomposites are clays. There are many distinct types of clays, each with its special properties, including exfoliation and swelling as well as variations in structure and composition (15).

1.1.1 The World of Clay and Clay Mineral

Clay is a naturally occurring substance made mostly of fine-grained minerals that become elastic in the presence of water and rigid when dried or burned, according to the Clay Minerals Society (CMS) and Joint Nomenclature Committees (JNCs) of AIPEA, expanded as the Association Internationale pour l'Etude des Argiles. However, it was noted that the term "clay" is used to refer to minerals (12).

But we should concur with the JNCs that 'clay' and 'clay mineral' should be distinguished clearly and clay should not be only referred to as a mineral. Regarding the use of clay as a rock word, the JNCs' stance is still unclear. Thus, we conclude that the term "clay" can refer to a rock, a sedimentary deposit, and the byproducts of primary silicate mineral weathering. This is based on historical usage. The titles "ball clay," "fire clay," "bentonite," "bleaching earth," and "fuller's earth" have all been used in literature in one form or another. It is important to always remember the differences between the terms clay and clay mineral. Despite this, because the term "clay" is shorter and less complicated than "clay mineral," it is frequently used in the literature. This report focuses on clay minerals instead of clays.

1.1.2 Clay Structure

Clays are layered silicates, composed of stacks of hydrated aluminosilicates with a minimum thickness of 1 nm and lateral dimensions ranging from 50 to 1000 nm. Their basic building blocks are octahedral sheets with eight oxygen atoms, enclosing a metal like aluminum, and tetrahedral sheets with four oxygen atoms surrounding silicon. The tetrahedral and octahedral sheets are connected by the exchange of oxygen atoms. Tetrahedral and octahedral sheets usually stack in a specific ratio and mode to form 1:1 layered silicates, which are also referred to as phyllosilicates.
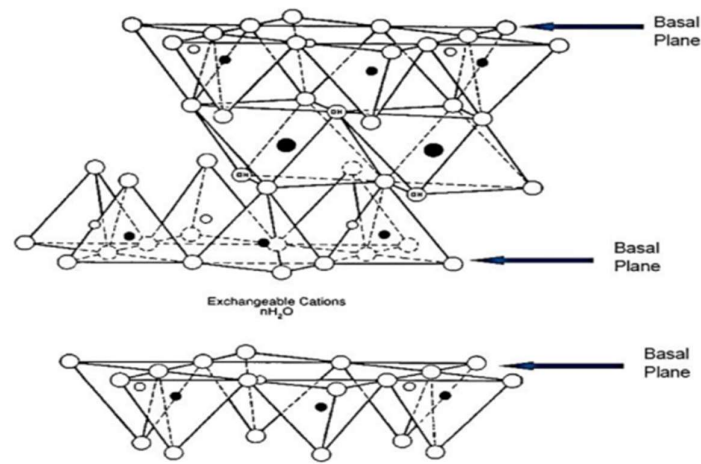
Fig.1.3 Diagram of clay layers and sheets

Phyllosilicates can be seen in clay layers, which are made up of tetrahedral sheets with four oxygen atoms, around a metal such as magnesium or aluminum and octahedral sheets with eight oxygen atoms surrounding an atom of silicon. Oxygen atoms bind the octahedral (O) and tetrahedral (T) sheets together. In the hydroxyl form, the oxygen atoms are not shared. The majority of the clays have two main Tetrahedral and Octahedral layer combinations (16). The kaolin group is one such combination. Here the kaolin group is made up of one octahedral and one tetrahedral fused (1:1). An octahedral sheet and a tetrahedral sheet fuse together to form the 1:1 layered structure known as the kaolin group. The layers are 0.7 nm thick and typically consist of $Al_2Si_2O_5(OH)_5$ with oxygen atoms shared.

On the other hand, a central alumina octahedral sheet is fused by the tip to two external silica tetrahedra in the 2:1 layered silicate crystal lattice, also referred to as 2:1 Phyllosilicate. This means that the oxygen ions in the octahedral sheet are also a part of the tetrahedral sheets (15). The following figures illustrate the composition of alumina and silica sheets.
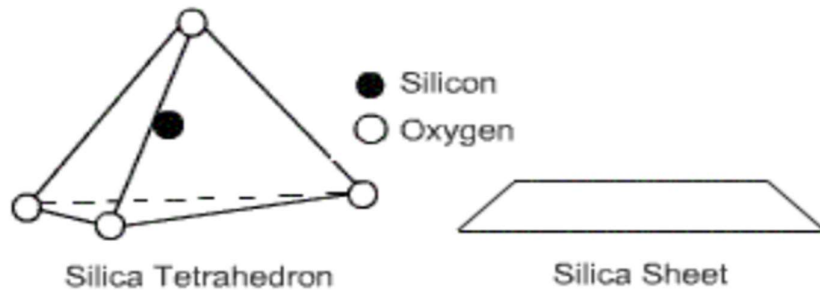
Fig.1.4 Silica Sheet
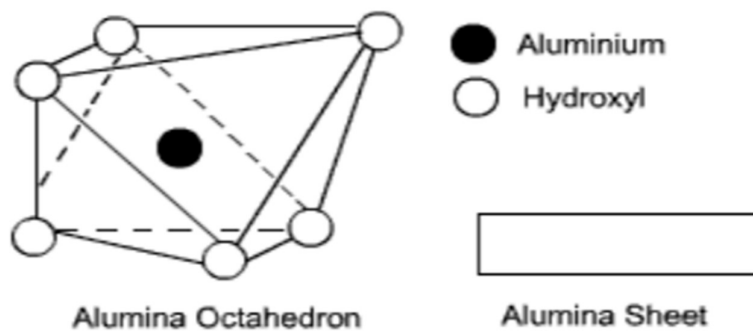
Fig.1.5 Alumina Sheet

Depending on the type of silicate particles, the clay used, and the manufacturing process, the layer's lateral dimensions can range from 300 Å to several micrometers or even larger, with a thickness of about 1 nm. As a result, these layers have an exceptionally high aspect ratio (length/thickness ratio) with values above 1000. Phyllosilicates are composed of one octahedral sheet sandwiched between two tetrahedral sheets (2:1), with a total thickness of 0.94 nm (17).

Two tetrahedral layers (MO_4) that create alternate T: O: T and a center layer with an octahedral symmetry of $MO_4(OH)_2$ combine to form a smectite clay

9

group. Bivalent magnesium or iron cations partially replace the aluminum cations found in the octahedral layer. Pyrophyllites are electrostatically neutral structures with a simple 2:1 configuration that don't contain interlayer ions. Since no ions are separating these layers, they do not expand in water. Consequently, pyrophyllite has almost no interior surface and just an exterior surface.

Clay swelling is the process by which cations that are present between the layers might become hydrated in the aqueous solution as a result of the interlayer spacing, i.e., the distance between the layers and the weak forces that exist between them. The interlayer gap is further increased, by swelling. For various clay groups with various clay structures, the charge density of clay layers varies (18). Due to the interlayer spacing and the weak forces between the layers, other molecules can also become embedded between the layers, especially in the hydrated state, leading to the expansion of the layer lattice and ultimately to the separation of the individual layers.

A layer is an arrangement of sheets that repeats itself regularly, such as tetrahedron-octahedron otherwise tetrahedron-octahedron-tetrahedron. A monolayer structure with two tetrahedral layers on either side of an octahedral layer made up of shared apical oxygen atoms is what distinguishes smectite, mica, vermiculite, talc, and pyrophyllite (19). One oxygen atom of the octahedral layer is located in the center of each ring and is protonated to provide the structural hydroxyl group because the oxygen atoms at the summit of the tetrahedral layer frame either hexagonal or ditrigonal rings. Charge imbalance within the layers of 2:1 layered silicates can result from the isomorphic substitution of cations with differing valencies. Charge imbalances of the opposite kind in neighboring sheets can

help to partially balance these (for example, a positively charged octahedral layer has a negative charge linked with a tetrahedral layer).

T

O

T $d_0 \sim 1.25 - 1.5$ nm

Exchangeable cations and $n \cdot H2O$

T

O

- $\bullet$ O
- $\bullet$ OH
- $\bullet$ Al, Fe, Mg
- $\bullet$ Si, Al
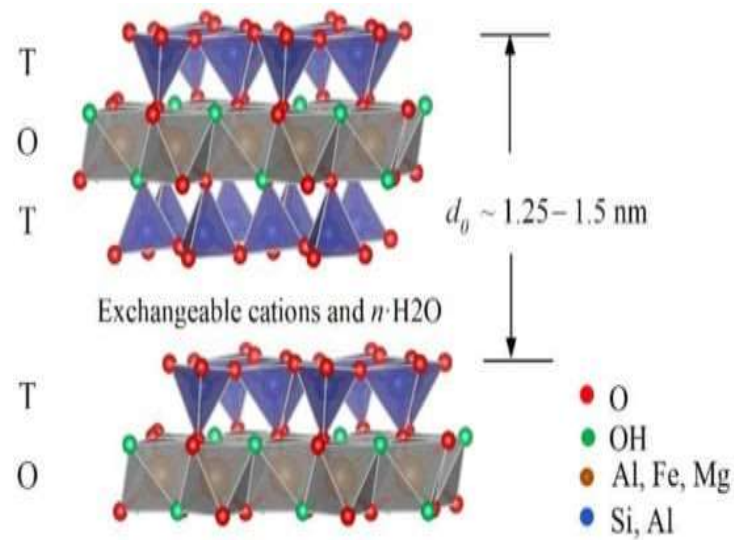
Fig.1.6 The structure of 2:1 type clay

1.1.3 Classification of clay

Clays can be classified based on their arrangement as 1:1 and 2:1 types of clays. Smectites come under the class of 2:1 clay. Montmorillonite is an important example of Smectite clay.
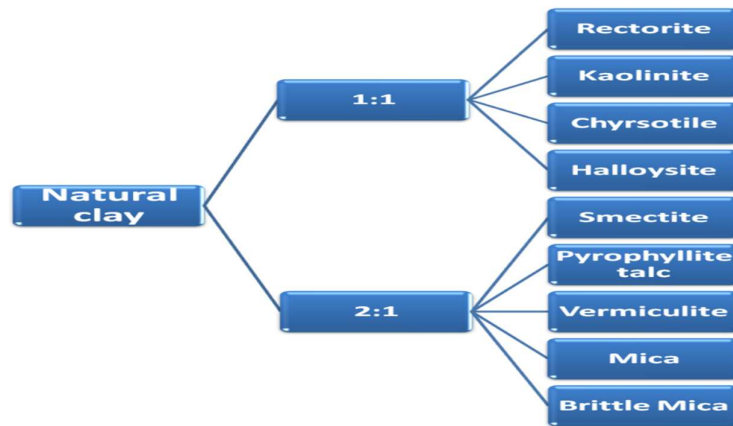
Fig.1.7 Classification of Natural Clay
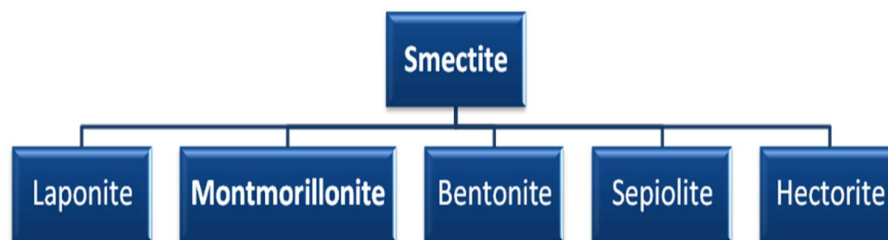
Fig.1.8 Classification Smectite

1.1.4 Properties of Clay

- **Cation Exchange Capacity:** To help with maintaining nutrients and rejuvenation applications, montmorillonite may exchange cations including calcium, magnesium, sodium, etc.

- **Swellability**: When exposed to water, swell ability causes a substantial expansion. It is therefore useful for absorption and sealing.

- Composed of layers of alumina and silica sheets. This permits ions and water to move between the layers.

12

- **High surface area**: provides a large number of locations for chemical reactions and adsorption.

- **Plasticity**: It is extremely moldable under damp conditions, making it suitable for molding and industrial use.

- **Water retention**: effectively holds onto moisture it helps with soil management and agriculture.

- **Thermal stability:** Beneficial for high-temperature applications and building materials because it preserves structural integrity at moderate temperatures.

- Layered structure with dimensions in the nm range and the anisotropy of the layers.

- The 1: 1 (T:O) layer thickness is approximately 0.7 nm, 2: 1(T:O) layer thickness is approximately 1 nm.

- **Low Permeability:** Serves as an organic defense against impurities and water. Utilized in construction and the maritime industry.

- The presence of several types of surfaces: external basal (planar) and peripheral surfaces as well as internal (interlayer) surfaces.

- The ease with which external and often internal, surfaces can be modified (by adsorption, ion exchange, or grafting).

- Shrinkage-swelling behavior involves the soil expanding when wet and contracting when dry, which impacts stability and structural changes.

1.2 MONTMORILLONITE (MMT)

Montmorillonite is a naturally occurring, very fine mineral of the smectite group of clays and it has a 2:1 layer structure that is made up of two silica tetrahedral sheets and an octahedral alumina sheet (T:O:T). This particular structure confers upon montmorillonite a permanent layer charge, high surface area, high thermal strength, and also superior cation exchange capacity. Montmorillonite clay (MMT), which is one of the widely used source materials for nano clay, finds extensive application across many sectors based on its better adsorption and intercalation characteristics.

Montmorillonite expands to many times its initial size when it is brought into contact with water. Their cation exchange capacity is high and their specific surface area is extremely high. There are interlayer gaps between each triple-sheet layer in montmorillonite, which is completely different from other clay nanoparticles. MMT is made up of the chemical substitution of Al^{3+} for Si^{4+} in the tetrahedral layer and Mg^{2+} for Al^{3+} in the octahedral layer. Because of this configuration, cations in the interlayer gaps balance the negative residual charge of montmorillonite. Water and a range of chemical and inorganic compounds can be absorbed by montmorillonite due to its special structure. It facilitates easy expansion and dissemination. A significant degree of thermal stability, the capacity to combine with other chemicals or polymers, as well as mechanical strengthening qualities (20). It is therefore a perfect part of nanocomposites for the process of absorption and environmental repair.

1.2.1 Intercalation capacity

In montmorillonite (MMT) molecules, ions, or polymers are positioned in between layers. This greatly boosts productivity at work. The method makes use of MMT's special layer structure, in which organic and inorganic species can be added to or substituted for exchangeable cations like Na^+ or Ca^{2+}, which hold the negatively charged silicate layer together. Which increases the separation between layers and enhances material compatibility. Cohesion improves MMT's contact, adsorption, and diffusion with other substances. Therefore, it is a useful instrument in the synthesis of nanocomposites (21).

1.2.2 Cation-exchange capacity

The ability of clay minerals to adsorb and adhere to specific cations and anions around the exterior of structural units is determined by the absence of positive or negative charges in their mineral structure. Absorbed ions are substituted by other ions. Quantitative relationships between interacting ions distinguish exchange reactions from simple sorption. The number of cations retained on the surface of soil particles is measured by the cation exchange capacity (CEC). It is defined as the number of cations that can be exchanged for other cations at a given pH and is often expressed in milliequivalents per 100 grams of dry clay.

Negatively charged ions on the surface of soil particles can combine with positively charged ions and exchange with other positively charged particles in the surrounding soil water, resulting in chemical changes in the soil. CEC affects several areas of soil chemistry. CEC measures soil fertility as it indicates the soil's ability to store nutrients such as K^+, NH_4^+, and Ca^{2+}. It also refers to the ability to retain environmentally harmful cations such as Pb^{2+}.

15

Because CEC is influenced by particle size, crystallinity, and adsorbed ions, the value of CEC for a particular mineral lies within a range rather than a single specific value. The exchange capacity is also pH-dependent due to the presence of hydroxyl groups on the surface of certain clay minerals such as allophane and kaolinite. The adsorbed cations displace or replace the initial negatively charged layer. This capacity of colloidal particles, such as clay minerals, to hold and trade positively charged ions is vital since it affects the mobility of positively charged species in soils and the overall geochemical cation cycle. CEC is a reversible process commonly associated with clay minerals due to the presence of exchangeable cations between the layers.

1.2.3 Swelling capacity

Upon addition of water to the dry clay minerals which is taken in a closed system, water is taken up in separate layers, causing expansion in the interlayer spacing. This occurs due to water-related energy forces, including hydrogen bonding, van der Waals interactions, and electrostatic effects, which influence particle interactions, stability, and dispersion in aqueous environments. With varying moisture content, clay minerals tend to experience large volume changes. The degree of swelling depends on several factors, including the charge density of the clay mineral layers, the nature of interlayer cations (monovalent or divalent), the concentration of ions in the surrounding solution, and the total composition of the clay minerals.

1.3 STARCH

Naturally occurring biopolymer molecules, starch has drawn a lot of interest because of its availability. A linear chain of glucose units called amylose and amylopectin make up the two primary components of starch. Due to its distinct qualities and uses, starch is a valuable substance for use in food, medicine, packaging, and environmental sustainability. Starch's physical and chemical characteristics make it extremely valuable. The starch polymer holds great promise as a substitute for components derived from petroleum (5).

Starch is regarded as being one of the most potentially useful natural polymers due to its alluring availability, affordability, and performance combinations. A polymeric carbohydrate made up of several glucose units connected by glycosidic linkages is called starch or amylum. The majority of green plants synthesize this polysaccharide to store energy. It is the most prevalent carbohydrate in the human diet globally and is found in significant quantities in staple foods like rice, cassava, corn, wheat, and potatoes. The Germanic origin of the term "starch" yields the meanings "strong, stiff, strengthen, stiffen." A white, without scent, tasteless powder is pure starch that is insoluble in alcohol or chilled water. It is made up of two different kinds of molecules: branched amylopectin and linear and helical amylose. By weight, starch typically comprises 20–25% amylose and 75–80% amylopectin depending on the plant. Starch is processed in industry to create a large number of the sugars found in processed meals. The majority of starches can be combined with warm water to form pastes. Wheat paste is one type of paste that can be used as a glue, thickening, or stiffening agent. The primary industrial non-food use of starch is as an adhesive in

papermaking. Before ironing, a starch solution can be used to stiffen certain textile materials.

Given its low cost, broad availability, and renewable nature, starch is the most preferred natural polymer resource for synthesizing nanocomposite. Higher plants primarily store carbohydrates as starches, which are plentiful and reasonably priced biopolymers. They can be generated continuously without worrying about running out of resources because they carry solar energy that has been stored (23). A novel family of materials with possibly better mechanical qualities is biopolymer-clay nanocomposites. Minimal quantities of clay are added to the biopolymer mix to create these kinds of composites (24).

Several drawbacks, including insolubility in water at room temperature, restrict the industrial use of naturally occurring starch. This restricts its applicability in formulations that need to dissolve or disperse right away. Different environmental conditions can cause them to break or lose their structural integrity like changes in temperature or extended storage. These restrictions are employed to enhance starch's qualities and increase its industrial uses. The creation of chemically modified starches has been a significant advancement in this area. It has shown itself to be a material with enhanced performance qualities and versatility. It can be used as an adsorbent to extract heavy metals and dyes from wastewater among other applications. Through chemical alteration, it is possible to optimize starch to improve its stability, affinity, and absorption of different contaminants. This results in an eco-friendly and effective way to stop pollution in the environment because it combines the efficiency needed for efficient water treatment with the advantages of a renewable resource (25).

1.3.1 Tapioca Starch

Tapioca is a starch made from cassava root a tuber that is native to South America. Cassava root is a staple meal in many countries in Africa, Asia, and South America and it is relatively easy to grow. Tapioca's almost pure starch contains almost all of its minerals. The starch obtained from tapioca is distinct from all other starches due to its exceptionally high molecular weights of amylose and amylopectin, minimal number of residual materials, and reduced amylose content when compared to other amylose-containing starches (26). For people on a gluten-free diet, it can be used in place of wheat in baking and cooking because it is naturally gluten-free. Dry tapioca is commonly sold as pearls, flakes, or white flour. A starchy liquid is extracted from powdered cassava root. Once the starchy liquid has been eliminated, the water is then left to evaporate. After the water evaporates completely, we are left with the tiny tapioca flour (27).

Fig.1.9 Cassava Starch

The cassava plant (Manihotesculenta) produces cassava starch, a highly nutritious, environmentally friendly, and renewable biopolymer from its

roots. In the field of polymer clay nanocomposites, it holds great promise in special qualities like a high amylose content and strong film-forming capabilities that work with a variety of materials. It is a strong contender for the creation of nanocomposite materials due to its exceptional durability and outstanding performance. Cassava starch nanocomposites show enhanced mechanical and thermal insulating qualities when mixed with clay nanoparticles like montmorillonite (MMT). Because of this, it can be used for a wide range of purposes. including environmental protection.

1.4 CHITOSAN

A naturally occurring biopolymer, that is easily biodegradable and biocompatible is chitosan, which comes from chitin. After cellulose, it is the second most prevalent polysaccharide found in nature. The exoskeletons of insects, crustaceans, and fungi contain chitosan. The process of deacetylating chitin yields chitosan. In order to expose the reactive amino group, the acetyl group must be removed.
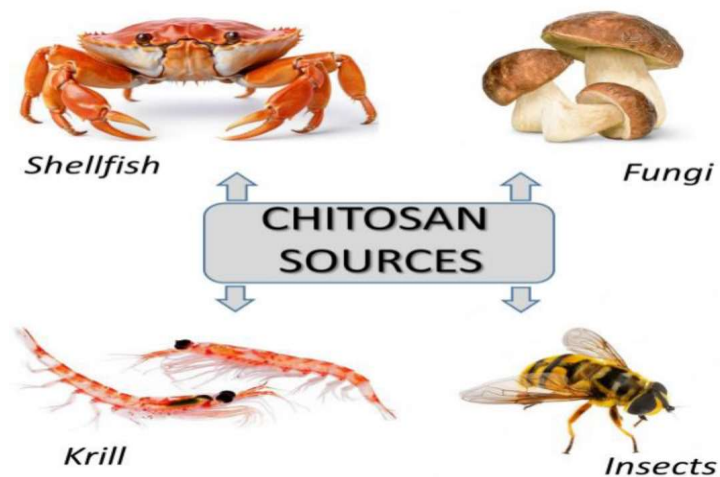
Fig.1.10 Sources of Chitosan

The polymer is made up of units. The distinct chemical structure of β-(1→4)-linked D-glucosamine and N-acetyl-D-glucosamine units. The properties of environmentally friendly Chitosan make it a priceless tool for tackling global issues about materials, innovation, and sustainability. Chitosan's special qualities are widely recognized in the areas of biodegradability, biocompatibility, antimicrobial activity, and film-making capabilities (28). Living organisms can metabolize glucosamine, one of the innocuous byproducts of chitosan's biodegradation. It is safe for use in pharmaceutical and biological applications due to its biocompatibility. The reason for this is that it doesn't trigger a strong immunological reaction. In a solution that is acidic through interactions with charges that are negative bacterial and fungal cell membranes, chitosan's amino protosan group adds to its antibacterial effect. Growth inhibition and disintegration result from this. However, the pH-dependent solubility of chitosan restricts its application in basic or neutral conditions. Chemical alteration is one way to get around this disadvantage. It makes mechanical strength, Specific functionality, and thermal stability stronger. Consequently, the range of applications is increased.

In the past few years, chitosan-based adsorption agents have gained more attention in the treatment of water and wastewater because of their abundance, affordability, and richness in amino and hydroxyl groups (29). Despite being present in a limited number of different types of mushrooms, chitosan is primarily produced as a byproduct of chitin using an alkaline deacetylation process that is carried out in an industrial setting since it is inexpensive and readily available (30).
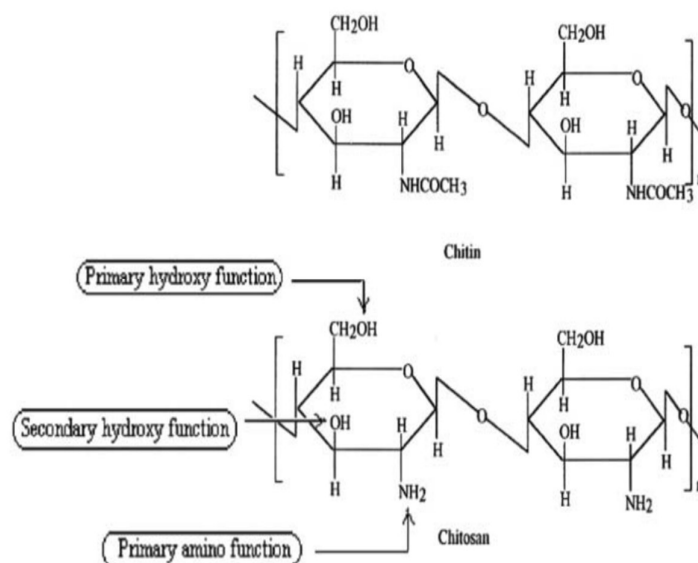
Fig.1.11 Structure of Chitin and Chitosan

Novel components known as chitosan-clay nanocomposites incorporate the special qualities of clay nanoparticles like montmorillonite (MMT) and the naturally degradable biopolymer chitosan (31). These materials have a variety of uses in industrial, health care, and environmental processes. Chitosan-clay nanocomposites tackle important issues related to innovations in technology and conservation. The chitosan matrix is strengthened by the aggregation of clay nanoparticles, increasing its flexibility and tensile strength. This improvement establishes a connection between the soil's silicate layer and the amino groups in chitosan.

1.5 THE HARMFUL IMPACT OF DYES

Fabric dyes are crucial in creating the variety and color of the clothing we wear daily. However, the frequent and extensive negligent discharge of these dyes into waterways has resulted in serious risks to the environment and public health. The textile business uses a lot of chemicals and water.

Large amounts of untreated or insufficiently treated dyes are dumped into lakes, rivers, and seas. Additionally, tainted water supplies present a major health concern to people. The clothing sector uses reactive dyes extensively due to their straightforward dyeing processes. These dyes are distinguished by azo linkages (N=N), and the related chromophores give the dye its color producing an extremely colorful effluent. Reactive dye discharges must therefore be treated before being released into the environment (9).

Since the dye is always concentrated, even in aqueous solutions at incredibly low concentrations it is visible (32). Dye particularly artificial dyes include chemical substances with mutagenic and carcinogenic qualities. Carcinogens are chemicals that encourage unchecked cell proliferation, which can lead to cancer. On the other hand, mutagens result in genetic mutations that cause several health issues including hereditary illnesses and birth abnormalities. As a result, these color's widespread presence in water sources poses a double risk to human health and the ecosystem (33).

Although dyes are not biologically reactive, numerous studies have demonstrated that when dye molecules are coupled with intestinal microbiota microorganisms and enzyme function, they can generate highly poisonous aromatic amino groups that can cause cancer (34). Many disorders, including tremors, dizziness, cyanosis, jaundice, diarrhea, vomiting, allergy issues, skin irritation, and nausea, can be brought on by dyes entering human food chains (35).

The natural dye alizarin red (1,2-dihydroxy-9,10-anthraquinone) is derived from the madder tree. Its chemical structure has allowed it to be employed in textiles from ancient times. They are frequently used in industry and contain hydroxyl groups. Without the use of adhesive chemicals, these

23

groups improve the dye's water solubility and offer silk and wool good stickiness. However, colors based on anthraquinone, including alizarin, are frequently discovered to be quite persistent contaminants. Usually, the textile industry releases them into aquatic environments. Their lack of concern leads to significant environmental issues (36).

1.6 POLYMER-CLAY NANOCOMPOSITE

Polymers are mixed with either natural or synthetic clays to generate polymer clay products. The addition of clay to polymers enhances their mechanical, thermal, barrier, and fire resistance qualities. The term "polymer-clay nanocomposites" (PCNs) refers to polymer-clay structures that have at least one phase having a texture at the nanoscale.

Due to their frequently distinct physical and chemical characteristics from those of pure polymers and traditional micro composites, nanocomposites offer enormous promise for use as highly useful materials. It should be noted that the primary characteristics of polymer-clay composites are heavily influenced by the adhesion between the surface's forces between the nanocomposite components, nano size, and the physical and chemical characteristics of the individual components. Clay is a common inorganic nanofiller used in common thermoplastics including nylon, polypropylene, polyethylene, and polystyrene because it is inexpensive, naturally occurring, and has a broad range of commercial applications (37).

Polymer nanocomposites offer outstanding qualities including strength, toughness, and fire resistance that greatly outweigh those of ordinary nanocomposites and are equal to metals, they have garnered a lot of attention. Additionally, PCNs are frequently used in industry as high-performance structural materials (38),(39),(40). The development of polymer-clay nanocomposites is now accelerating because of advancements

24

in matrix polymer, mechanical and thermal characteristics as well as the potential to dissolve polymers and clays without the use of organic solvents. The dispersion of nm thick clay layers within the polymer matrix is what causes this enhanced quality (41).

With currently available manufacturing equipment, PCNs may be shaped into intricate designs because the nano-dispersed clay layer lowers the permeability of the polymer matrix. PCNs can also be utilized in storage tanks and packaging applications. Since nanometer-scale silicate layers scattered throughout the polymer matrix frequently give rise to notable thermal, mechanical, and barrier properties. Polymer-clay nanocomposites have garnered a lot of attention during the past 20 years.

According to reports, nanocomposites with various morphologies, structures, properties, and uses can be created by adjusting the polymer–clay interaction. These polymer-clay composite's recent developments in terms of self-assembly and the creation of various morphologies have also made it possible for them to be used as extremely useful materials in controlled delivery systems (42). The existence of nanoscale phases has significant effects in addition to improving the mechanical, thermal insulation, durability, chemical stability, flame retardancy, scratch, abrasion resistance, biodegradability, optical, magnetic, and electrical properties of polymer bulk phases. The interfacial contact between the clay and the polymer is one such effect. Aspect ratio and clay content have an impact on how well nanocomposites operate mechanically.

Recently, polymer-clay nanocomposites have grown in popularity because of their comparatively modest percentage of qualities that are noticeably better than those of conventional polymer composites. Two aqueous solutions containing monomers can be immediately mixed with a clay

25

suspension to create polymer-clay nanocomposites. Polymers can be produced by induction with heat, light, or by adding polymerizing agents. Since most of the polymer is located outside the clay interspaces, the finished product is known as an ex-situ nanocomposite.

Notably, the initial concentration of clay can be changed and in certain situations, the clay layers can be fully separated. Consequently, the result in this case is known as an exfoliated polymer-clay nanocomposite. The second method involves adding monomers to the clay interlayer space through diffusion or charge exchange inside clay galleries that have already been altered with organic salts. The embedded polymer can be polymerized to produce so-called in-situ nanocomposites because the majority of the polymer content is found in the clay's interstices.

1.6.1 Polymer clay nanocomposite structure

The structure of polymer–clay nanocomposites is often categorized based on the extent to which polymer chains are inserted and exfoliated into clay galleries. Numerous elements, including the type of clay, organic modifier, polymer matrix, and manufacturing technique, affect the extent of insertion and exfoliation.

As a result, various composite microstructures can be designed and tailored depending on the type and quality of the clay and polymer. The specific processing technique used to fabricate the nanocomposite which influences factors like particle dispersion and overall structural integrity (43).
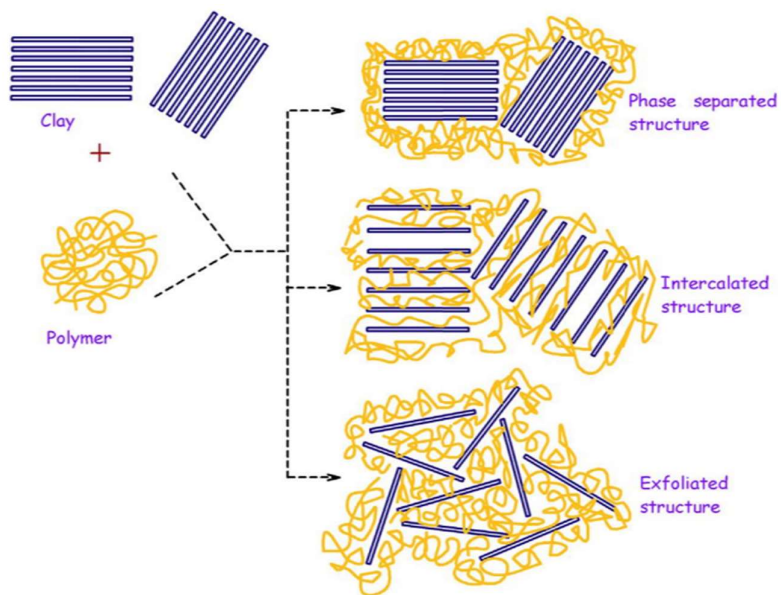
Fig.1.12 Different types of polymer clay nanocomposites

1.6.2 Classification of PCNs

There are three forms of PCNs that can be produced thermodynamically, depending on how strongly the polymer matrix and layered silicate interact.

1.6.2.1 Intercalated Nanocomposite

If one or more polymer chains are introduced into the interlayer space, increasing the interlayer distance while maintaining the periodic arrangement of clay layers, the result is an intercalated nanocomposite. The electrostatic interactions between the layers are lessened but not eliminated by the presence of polymer chains within the galleries. With strong interfering interactions between the clay layer and polymer chains, this combination produces an ordered multilayered hybrid morphology.

1.6.2.2 Phase-separated Nanocomposite

The clay is dispersed as layered aggregates or particles in the polymer network when an organic polymer intercalates into an inorganic clay (unmodified clay), preventing the polymer from intercalating into the clay layer. Phase separation is the term used to describe the final composite structure. Phase-separated polymer-clay composites have characteristics that are comparable to those of traditional nanocomposites.

1.6.2.3 Exfoliated Nanocomposite

Polymer chains are inserted into clay galleries to create layers that are separated from one another. When the separate layers are distributed across the polymer matrix, an exfoliated or delaminated structure is created. Exfoliated structure is produced when the interlayer gap between the polymer chains is increased by more than 80–100Å. A high aspect ratio and a low necessary clay content in the exfoliated nanocomposite are the results of the individual clay layer's excellent dispersion. Additionally, the clay and polymer's extensive surface contacts greatly enhance the polymer's characteristics.

1.6.3 Properties of PCNs

When compared to pure polymers, nanocomposites made up of polymers and layered silicates essentially have improved mechanical and material properties. Enhancements include decreased gas permeability and flammability, as well as increased modulus strength and heat resistance. Additionally, these composites have superior biodegradable qualities. Additionally, PCNs exhibit enhancements in the most prevalent polymer characteristics. Apart from decreased gas and liquid permeability, the nanocomposites also show notable enhancements in solvent absorption.

Another characteristic that is greatly enhanced by the usage of stacked silicates is scratch resistance. When compared to conventional filler-reinforced systems, the stronger interfacial interaction between the matrix and the silicate is the primary cause of these benefits.

1.6.3.1 Temperature Durability

Clay has been demonstrated to increase thermal stability by serving as an excellent mass transport barrier and insulator for volatile compounds produced during decomposition when incorporated into the polymer matrix. It was discovered that clays occasionally caused the early phases of pyrolysis to occur at greater temperatures. The heat barrier effect of the laminated silicate layer, which retains the collected heat, also caused a reversal of thermal stability. This might be utilized as a heat source to quicken the decomposition process in combination with the heat flux supplied by the external heat source.

1.6.3.2 Mechanical Properties

The interaction between the dispersed clay nanoparticles and the polymer matrix results in improved mechanical characteristics for polymer clay nanoparticles. The strength, hardness, and durability of the material are significantly increased by the nanoscale distribution of clay platelets within the polymer. When stacked silicates were used to create the nanocomposites, the polymeric material's tensile and flexural qualities significantly improved.

1.6.3.3 Adsorption Capacity

Nanocomposites of polymer clay are well known for their superior absorption capabilities. Because of this, it is very successful at eliminating pollutants from aqueous solutions, including dyes, heavy metals, and

organic contaminants. Clay nanoparticles and polymer matrices work in concert to increase the adsorption capacity by improving surface area, functionality, and porosity. The total surface area of the nanocomposite is greatly increased by the dispersion and slippage of clay nanoparticles within the polymer matrix. There are several active areas on this large surface for adsorbing contaminants. The dispersion and slippage of clay nanoparticles inside the polymer matrix significantly increase the nanocomposite's overall surface area. This broad surface has multiple active zones for adsorbing pollutants.

1.6.3.4 Heat Distortion Temperature (HDT)

A polymeric material's HDT is a measurement of how resistant it is to heat under applied loads. For any polymeric material, the rise in HDT brought on by clay dispersion could be an incredibly important property upgrade. Using traditional fillers to produce comparable HDT improvements is quite challenging.

1.6.3.5 Fire Retardant Properties

The development of high-performance silicate material with carbon char that builds up on the surface during firing is responsible for the enhanced flame-retardant qualities seen in nanocomposites. This reduces the mass loss of breakdown products and isolates the underlying substance.

1.6.3.6 Biodegradability

The notable increase in biodegradability following the creation of nanocomposites is another intriguing and thrilling feature of PCNs, most likely due to the catalytic function of organoclays in the biodegradation process (44).

1.6.3.7 Gas Barrier Properties

Clays are thought to improve barrier qualities by forming a convoluted or maze-like path that slows the passage of gas molecules through the resin matrix. The longer diffusive path that the penetrant must take when the filler is present results in a decrease in permeability.

1.7 KEY OBJECTIVES OF CURRENT STUDY

- To synthesize Starch-Montmorillonite Nanocomposite

- To synthesize chitosan-starch-montmorillonite (CS-MMT) nanocomposites at varying ratios of chitosan to starch-MMT

- To analyze and characterize the synthesized nanocomposites using FT-IR, XRD, and TGA techniques.

- To determine the adsorption capacity of the CS-MMT nanocomposites for reactive dyes from wastewater and confirm this via UV analysis.

Chapter 2

Literature Survey

Polymer nanocomposites have made the polymer nanocomposite industry all the more exciting, with the ability to control the tailoring of polymer properties more accurately. Based on Saheli Ganguly and others, "polymer nanocomposites" are hybrid systems that have one or more dimensions on the nanoscale incorporated into a polymer matrix (45). Through the addition of nanofillers, even at very low concentrations, the extent of improvement in polymer matrix properties can be quite remarkable.

The incorporation of nanofillers into polymer matrices has been widely reported to improve some important material properties, such as mechanical strength, thermal stability, and gas barrier properties, without sacrificing toughness or transparency and thus are perfectly suited for packaging applications. Additionally, layered materials have also drawn considerable interest as drug delivery vehicles due to the ability of layered materials to intercalate polar organic compounds between their layers and form versatile interlayer compounds. Controlled drug delivery from these drugs due to the intercalation of drugs situates them among potential candidates for drug applications (45).

As per Riya Mascarenhas and others, the introduction of nanocomposites during material preparation results in multiphase or single-phase glass, ceramic, or porous materials with upgraded properties. What is interesting about nanocomposites is that they have better characteristics than polymer

nanocomposites and pure polymers such as greater bond strength, lower gas permeability, and better thermal and mechanical properties (46).

The incorporation of inorganic compounds into polymers results in great improvements in several properties, such as mechanical strength, thermal stability, flame retardance, gas barrier properties, and corrosion resistance. Additionally, small additions of clay can cause intercalation or exfoliation, which can be identified through X-ray diffraction (XRD) methods. Exfoliated composites are particularly found to have significantly enhanced physical and chemical properties due to the large surface area and high aspect ratio of the clay (47).

Naturally occurring smectite clays are hydrophilic and their character is usually adjusted with quaternary ammonium salts to make them organophilic. Through this treatment, they become compatible with hydrophobic polymers, allowing the development of intercalated and exfoliated nanocomposites. Scientists persist in looking for thermally stable surfactants that can sustain the high thermal conditions needed in melt-processing thermoplastics (14).

Polymer clay nanocomposites are generally prepared by in situ polymerization, melt processing and solution techniques. The nanocomposites have superior mechanical and transport properties and are suitable for improving the performance of pure polymeric materials and even replacing some metals or composite materials. Incorporation of small quantities (typically <5% by volume) of appropriately pre-treated clays considerably improves the mechanical and barrier properties of polymers without affecting optical clarity. Additionally, the addition of clay can enhance the ionic and electrical conductivity of conductive polymers as well as the biodegradability of polymers. Importantly, the addition of a

small proportion of clay makes the resulting nanocomposite processable like unfilled polymers (14).

Among other nanofillers investigated for their reinforcing properties, clay materials have been researched widely as polymer matrix fillers to bring about significant property improvements. During the last decade, polymer-clay composites have attracted much interest based on their dramatic enhancements in mechanical properties, thermal stability, flame retardancy, gas barrier properties, and corrosion protection, better than conventional alternatives (14).

The word "clay" in fact covers layered silicates and clay minerals, namely aluminum layered silicates, with an accessory amount of metal oxides, like alkali metals, alkaline earth metals, and magnesium, together with organic materials (48).

Dispersion of clay in polymer matrices is challenging because of the strong covalent bonding between the layers of clay. To overcome this, scientists such as Syed Abusale Mhamad Nabirqudri and others have discovered that it is necessary to prepare the clay particles before dispersion in the polymer matrix.

The mechanism of interaction between the polymer and the clay is as follows: The cation of the metal on the clay replaces the carbocation of the surfactant and forms a long alkyl chain. This process increases the interface, resulting in better physical and chemical properties of the polymer-clay composite (47). These alterations facilitate the addition of hydrophobicity to the clay particles so that they can be well dispersed in the polymer matrix, thus improving the overall performance of the composite material (48).

Montmorillonite (MMT) is the most common clay mineral used in preparing nanocomposites because of its high cation exchange capacity (CEC). For modifying MMT, a two-step process is utilized, where sodium ions (Na^+) between the layered structures are exchanged with surfactants, monomers, or initiators. This basal space expansion allows for monomer penetration, before the polymerization process as described by Ahmed M. Youssef and others (49).

The addition of montmorillonite clay greatly improves the electrical and mechanical characteristics of composite materials. Therefore, the composites possess tremendous potential in a range of technological applications such as transistors, microelectronics, sensors and solar encapsulation material according to Syed Abusale Mhamad Nabirqudri and others (47).

Montmorillonite (MMT) facilitates the retrieval of nanostructures that can be used to design new and advanced packaging materials. By mixing MMT with well-known packaging polymers like polypropylene (PP), polyethylene (PE), polyethylene terephthalate (PET), and polystyrene (PS) nano clays with better mechanical, thermal, optical, and barrier characteristics can be synthesized. According to F. Vilarinho and others (48), this method can be used to produce composite films with enhanced performance.

Different techniques can be used to prepare polymer/clay nanocomposites, such as in situ polymerization, solution intercalation, melt intercalation, and sol-gel methods. The basic principle behind nanocomposite formation is to initiate a process of polymerization within the nm-scale interlayer region of the clay. With increasing polymer chains in this tight space, they expand the clay layers and either intercalate (partial basal space

expansion) or exfoliate (full isolation and dispersion of individual layers of clay in the polymer matrix) (49).

Clays are readily available and cheap and thus good adsorbents because of their layered structure. Their structure enables clays to be "hosting materials" for adsorbates and counterions. Studies have established that the surface of clays is packed with exchangeable ions, which are important in the environment by enabling the adsorption of cations and anions (50).

Clays possess high affinities for both cations and anions and therefore are very efficient in dye removal from wastewater. The pH-dependent variations in the adsorption capacities of clays have been proved through studies, and adsorption is largely controlled by ion-exchange processes. In a surprising twist, most dyes are of natural origins, (51) such as plants, insects, animals, and minerals without undergoing chemical treatment.

The biopolymer consisting of poly-b-(1,4)-2-amino-2-deoxy-D-glucose is the second most common naturally occurring biopolymer formed by the process of deacetylation from chitin. Chitosan is a readily available polysaccharide originating mainly from aquatic animals, like shellfish, crabs, and prawns.

Chitosan's cationic character makes it distinct from other polysaccharides, which are generally neutral or anionic. Under acidic conditions, the amino functional group (NH_2) of chitosan protonates to give NH_3^+, and this confers antimicrobial and antifungal activity.

The combination of the non-toxicity, biocompatibility, and antimicrobial activity of chitosan has made it common in several biological fields (52).

Chitosan's unique structure featuring multiple functional groups such as primary hydroxyl, secondary hydroxyl, and primary amino groups enables

36

it to interact more effectively with nanofillers compared to other polymer matrices (31). The intrinsic biocompatibility of nano-clay and chitosan renders their composites promising for different biomedical applications (53). Despite a wealth of research on the influence of montmorillonite (MMT) concentration in chitosan, little is known about the sorption behaviour of chitosan-nano clay (CN-MMT) nanocomposites with different nano clay concentrations.

Azo dyes are organic compounds with the functional group R−N=N−R′, where R and R′ are generally aryl and substituted aryl groups. They are a commercially important, family of azo compounds i.e. compounds having the C−N=N−C linkage and do not exist naturally (54). Responsible for 60-70% of all dyes utilized in food and textile production. Azo dyes find extensive use in textiles, leather, and foods. Azovarious pigments are also closely associated with azo dyes and are water-insoluble and insoluble in other solvents (55)(56).

Azo dyes control the production quantity of dye chemistry, and their significance is likely to increase. In recent times, azo-functionalized dyes containing aromatic heterocyclic compounds have been in focus due to their bright colors, luminosity, simplicity of production, and outstanding dyeing properties (57),(58),(59),(60).

Alizarin Red A, or Alizarin Red S, is a commonly used dye that is frequently employed for testing methods to remove dyes from wastewater owing to its brilliant color and the possibility of toxicity to the environment. Amongst the different technologies of treatment, adsorption has emerged as one of the good technologies for aqueous effluent treatments (61).

Different industries such as textiles, printing, paper, carpet, plastic, and leather production use dyes to give color to their products. These dyes, however, may stay in industrial waste and are then released into water bodies (62).

Dyes are pigmented substances commonly used in different industries, including textiles, printing, rubber, cosmetics, plastics, and leather, to dye their products. Such widespread application of dyes leads to the production of high volumes of colored wastewater. Dyes are mostly grouped into three classes: anionic, cationic, and non-ionic. Significantly, the textile industry is the biggest user of dyes for coloring fibers (63).

These dyes have serious environmental implications since they are very toxic and possibly carcinogenic to microbial communities and mammalian animals. It is thus critical to eliminate them from water effluents before disposal into water bodies. The light stability of dyes and their resistance to biological degradation and aerobic digestion render them especially difficult to eliminate from industrial wastewater (64).

Removing color from wastewater generated by textile and manufacturing industries poses a significant environmental challenge (65). This is because dyes are very soluble in water, with bright colors being produced, especially under acidic conditions. The textile sector alone consumes more than 10,000 commercially used dyes globally. Dye consumption by this sector every year is in excess of 1,000 tons of which about 10-15% of these dyes find their way into waste streams as effluents during dyeing (63).

Scientists are always on the lookout for more effective, cheaper, and easily available adsorbents, especially from waste products. Recently, composites like starch/clay (66) and chitosan/starch have been utilized for

38

the removal of reactive dyes from aqueous solutions. Yet, no research has reported the synthesis and use of a starch-montmorillonite/chitosan (St-MMT/chitosan) nanocomposite as an adsorbent for dye removal.

Considering the prospects of these materials in dye removal, our objective was to design a new nanocomposite that takes advantage of the synergistic or complementary attributes of starch, montmorillonite, and chitosan. We were interested in synthesizing and characterizing this three-component nanocomposite and determining its efficiency in removing reactive dyes from aqueous solutions (9).

Chapter 3

Materials and Methods

3.1 WORK PLAN

The main goals of our project were to prepare starch-MMT nanocomposite and to synthesize chitosan-starch montmorillonite nanocomposites by varying the ratios of chitosan to starch-MMT. The nanocomposites were characterized using FT-IR and XRD techniques and their thermal stability was assessed through TGA analysis. Furthermore, verified the adsorption capacity of the CS-MMT nanocomposites for removing reactive dyes from wastewater using UV analysis.

3.2 WORK CARRIED OUT

- Synthesis of Starch-Montmorillonite Clay nanocomposite.
- Synthesize chitosan-starch montmorillonite (CS-MMT) nanocomposites at varying ratios of chitosan to starch-MMT.
- Examination of the intercalation chemistry of the produced nanocomposites using FT-IR and XRD techniques.
- The thermal stability of different nanocomposites was assessed through TGA analysis.
- Evaluation of the adsorption capabilities of the nanocomposites for the removal of reactive dyes from wastewater using UV analysis.

3.3 EXPERIMENTAL PROCEDURE

3.3.1 Materials required

Sodium Montmorillonite clay with cation exchange capacity (CEC) 92.6mEq/100 g purchased from Southern Clay Products, USA. Cassava Starch, Chitosan, acetic acid, and distilled water.

Fig.3.1 Cassava Starch   **Fig.3.2 Chitosan**   **Fig.3.3 Na⁺-MMT Clay**

3.3.2 Synthesis of Starch-MMT Clay Nanocomposite

Weight of clay   = 2 g

Weight of Starch   = 2 g

Total volume of distilled water   = 200 ml

To create a 2% (w/v) solution, distilled water was used to dissolve 2g of starch (St). A separate solution containing the required concentration of Na⁺-MMT (2%, w/v) was made in distilled water and allowed to hydrate for a full day. After that, the dispersion was ultrasonically treated for five minutes. Under agitation, equal amounts of the clay dispersion and starch solution were combined at 40°C. After mixing the mixture for eight hours, it was transferred onto plastic Petri plates and allowed to dry naturally**.**

41
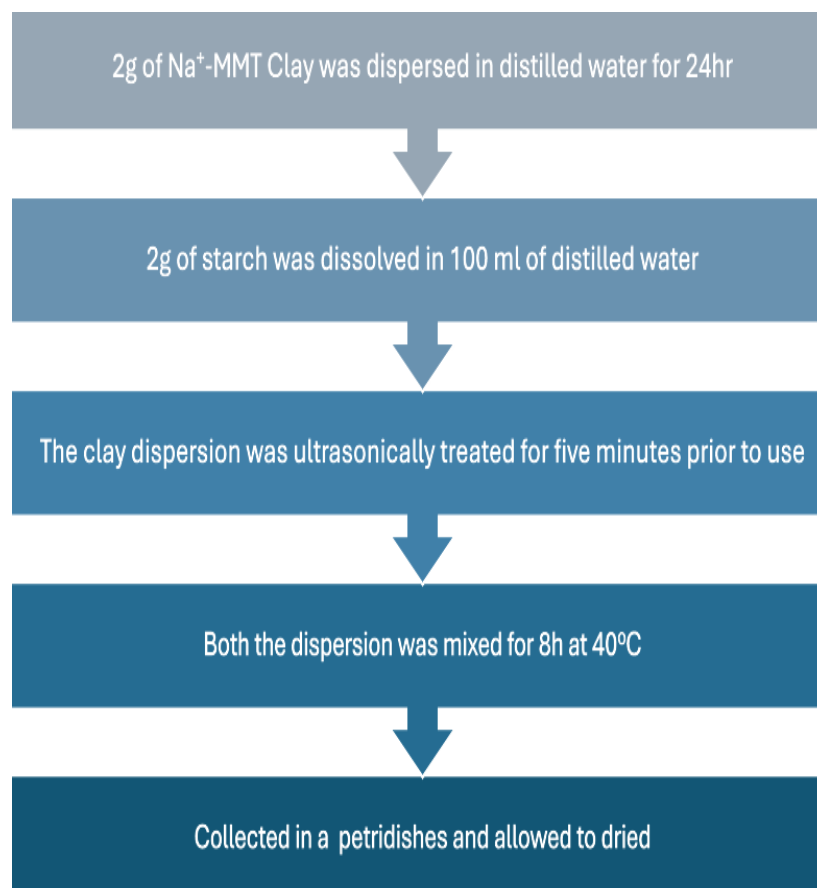
Fig.3.4 Flow chart for the synthesis of St-MMT nanocomposite

3.3.3 Synthesis of Chitosan Starch-MMT nanocomposite using 1x:0.1x Chitosan: St-MMT Clay

Weight of Chitosan $= 1$ g

Weight of Starch-MMT $= 0.1$ g

Volume of Acetic acid $= 1$ml

Total volume of distilled water $= 199$ ml

Initially, 100 mL of 1% (v/v) acetic acid was used to dissolve powdered chitosan of 1g, stirring for approximately two hours to create a transparent chitosan aqueous solution. Furthermore, 0.1g of St-MMT Clay was

42

dispersed in the distilled water and agitated for 12 hours prior to usage to produce a 0.1wt% suspension. At 60°C, the chitosan solution was thereafter gradually introduced to the existing clay suspension. Following two hours of stirring, the reaction mixture was spun through a centrifuge and rinsed three times with distilled water. After 12 hours of drying at 100°C, the nanocomposite materials were ground to power.

0.1g of St-MMT Clay was dispersed in the distilled water and stirred for 12hrs

1g of chitosan was dissolved in 1% (v/v) acetic acid and stirred for 2hrs.

At 60°C, the chitosan solution was gradually added to the St-MMT Clay suspension and stirred for 2hrs.

Reaction mixture was centrifuged alone and three times with distilled water.

The nanocomposite materials were dried at 100°Cand then ground to power.

Fig.3.5 Flow chart for the synthesis of Chitosan Starch-MMT nanocomposite using 1:0.1 Chitosan: St-MMT Clay

43

3.3.4 Synthesis of Chitosan Starch-MMT nanocomposite using 1x:0.5x Chitosan: St-MMT Clay

Weight of Chitosan   = 1 g

Weight of Starch-MMT   = 0.5 g

Volume of Acetic acid   = 1ml

Total volume of distilled water   = 199 ml

Initially, 100 mL of 1% (v/v) acetic acid was used to dissolve powdered chitosan of 1g, stirring for approximately two hours to create a transparent chitosan aqueous solution. Furthermore, 0.5g of St-MMT Clay was dispersed in the distilled water and agitated for 12 hours prior to usage to produce a 0.5wt% suspension. At 60°C, the chitosan solution was thereafter gradually introduced to the existing clay suspension. Following two hours of stirring, the reaction mixture was spun through a centrifuge and rinsed three times with distilled water. After 12 hours of drying at 100°C, the nanocomposite materials were ground to power.
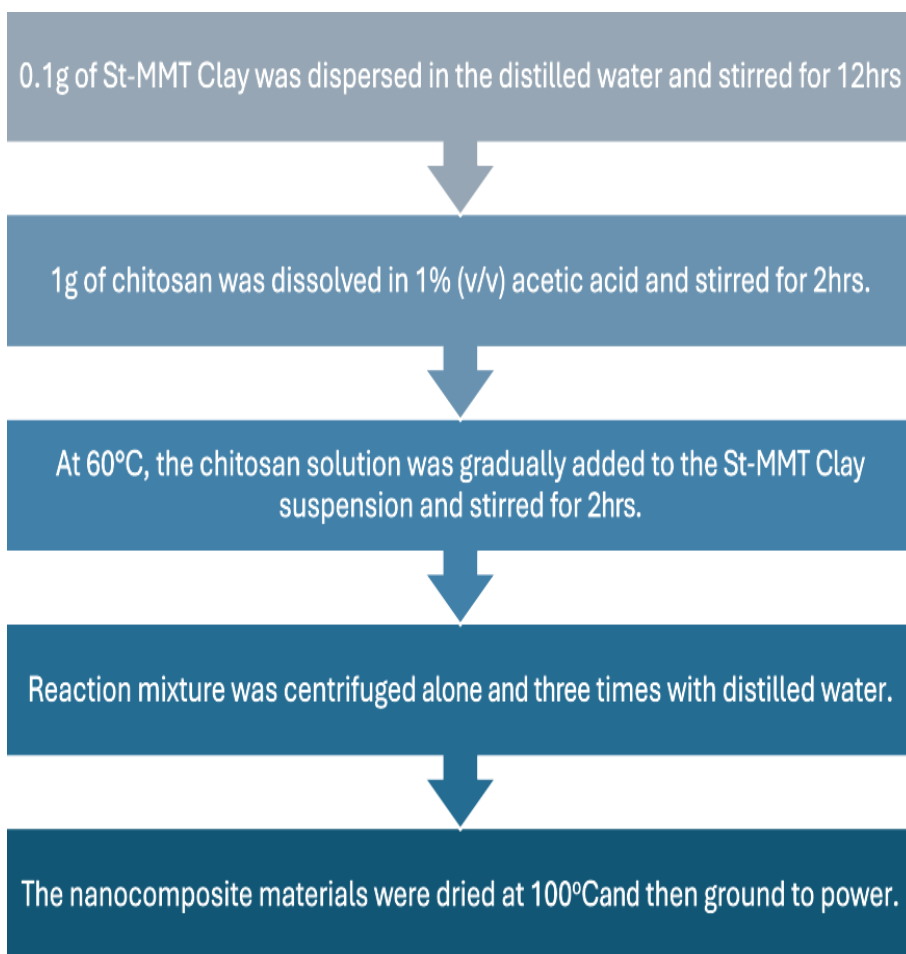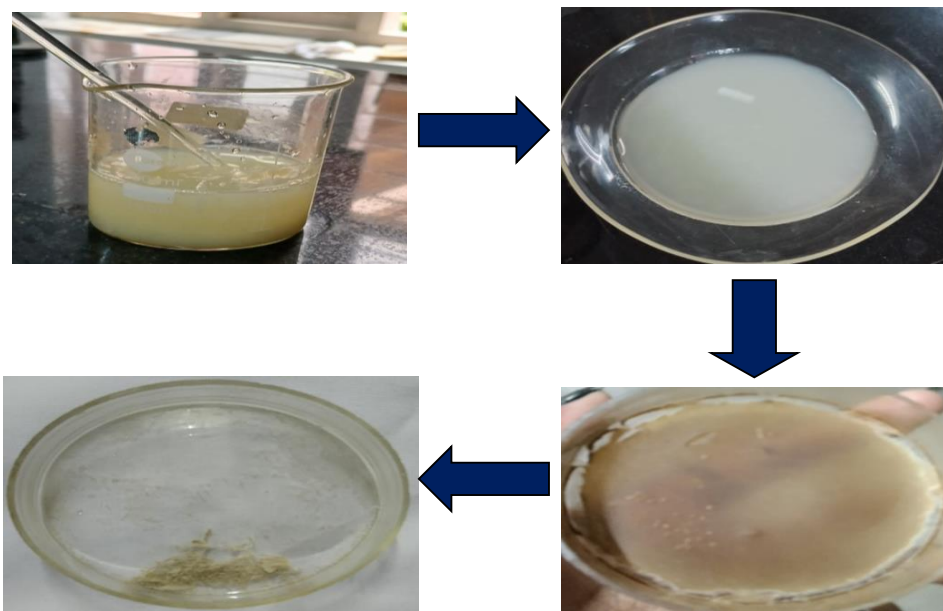

Fig.3.6 Preparation of Chitosan Starch-MMT nanocomposites

3.3.5 Synthesis of Chitosan Starch-MMT nanocomposite using 1x: 1x Chitosan: St-MMT Clay

Weight of Chitosan   = 1 g

Weight of Starch-MMT   = 1 g

Volume of Acetic acid   = 1ml

Total volume of distilled water   = 199 ml

Initially, 100 mL of 1% (v/v) acetic acid was used to dissolve powdered chitosan of 1g, stirring for approximately two hours to create a transparent chitosan aqueous solution. Furthermore, 1g of St-MMT Clay was dispersed in the distilled water and agitated for 12 hours prior to usage to produce a 1wt% suspension. At 60°C, the chitosan solution was thereafter gradually introduced to the existing clay suspension. Following two hours of stirring, the reaction mixture was spun through a centrifuge and rinsed three times with distilled water. After 12 hours of drying at 100°C, the nanocomposite materials were ground to power.

3.4 CHARACTERIZATION

Chitosan St-MMT nanocomposite's functional group characterization and d-spacing between the clay layers were investigated through FT-IR and XRD analyses.

3.4.1 Characterization using FT-IR

The newly prepared nanocomposites are subjected to FT-IR analysis. Using infrared spectroscopy, the molecular vibrations are investigated. Infrared light can only be absorbed by bonds that have a varying dipole moment during vibration. The samples of St-MMT Clay nanocomposite and Chitosan St-MMT nanocomposite with different ratios were characterized using FT-IR. The spectrum was obtained using KBr pellets

in the 4000cm^{-1} to 400cm^{-1} range. Percent transmittance is plotted against wavenumber. Certain groups inside the molecule produce characteristic absorption bands with wavenumbers that fall within a particular range, regardless of the composition. The wave numbers at which absorption is detected can be used to identify the presence of functional groups. In the current investigation, the intercalation of the modifiers in the clay was confirmed using infrared data.

3.4.2 Characterization using XRD

X-ray diffraction is a non-destructive analytical technique for identifying and characterizing the crystalline structure of materials. The technique relies on the principle of diffraction, which happens when X-rays interact with a crystalline material. The particular arrangement of atoms in the crystal lattice causes the X-rays to scatter in specific directions, thus producing a diffraction pattern that can be recorded and analyzed. X-ray diffraction uses the dual wave/particle duality of X-rays. This technique's primary use is the identification and characterization of substances according to the pattern of their diffraction. XRD is a potent analytical method for figuring out the interlayer spacing, phase composition, and crystalline structure of nanocomposites. The reflected X-ray intensity is plotted against 2θ values in the XRD graph.

where θ is the angle at which the X-ray strikes the sample and n is the order of reflection. Monochromatic X-ray wavelength is denoted by λ, while d represents the separation between two comparable planes. The d-spacing can be calculated using Bragg's equation. In the present study, the intercalation of clay was assessed by utilizing XRD to determine the angle of diffraction and d-spacing values.

3.4.3 Characterization using TGA

Using a Hitachi-STA 7300 TGA equipment, thermogravimetric analysis of the prepared samples was carried out at temperatures between 0-750°C. A thermal analysis method called thermogravimetric analysis (TGA) uses a controlled environment to evaluate a material's change in mass as a function of temperature or time. It offers important details regarding the composition, breakdown behavior, and thermal stability of materials. Adsorption, breakdown, evaporation, and oxidation are examples of physicochemical processes that TGA operates on. It frequently corresponds to a detectable shift in mass. As the sample undergoes a regulated heating and cooling program inside the furnace, its weight is continuously monitored by a sensitive balance. To accommodate the material qualities and analytical objectives, this process is carried out in particular atmospheric conditions, such as inert (such as nitrogen), oxidize (such as air) or reduce (such as hydrogen).

A typical procedure involves heating a sample steadily or keeping it at a particular steady temperature, where mass is continuously measured in relation to time or temperature. A heat-gravity graph, which plots mass loss (or gain) against temperature or time is created from the resultant data. This curve provides crucial information about the thermal behavior of a material including the temperature at which there is a noticeable shift in mass, stability, and decay time of different components.

3.4.5 UV-Visible Analysis

In the electromagnetic spectrum's visible (VIS) and ultraviolet (UV) regions which range from 200 to 800 nm, most organic compounds and functional groups exhibit little to no light absorption, making absorption spectroscopy less effective in this area. However, insights can occasionally be gained from these spectral regions. By integrating this

information with data obtained from infrared spectroscopy, significant structural insights can be uncovered. This concept is derived from Beer-Lambert's Law. When energy is absorbed by electrons in both bonded and unbonded molecules, they transition to higher energy states, and there are four main types of transitions: π-π^*, σ-σ^*, n-σ^*, and n-π^*. The hierarchy of energy for these transitions is as follows: σ-$\sigma^* >$ n-$\sigma^* > \pi$-$\pi^* >$ n-π^*. Absorption in the 200-260 nm range is attributed to the transitions, while n-π^* transitions are responsible for absorption in the 350-400 nm range. Ultraviolet-visible spectroscopy was conducted within the 200 to 700 nm range.

3.5 APPLICATION-DYE REMOVAL

3.5.1 Preparation of Dye solution

In order to create a 10 ppm Alizarin Red dye solution, 10 mg of Alizarin Red dye was first dissolved in 100 ml of distilled water to create a stock solution with a 100 ppm concentration. The stock solution was then utilized to make the required 10 ppm solution. Precisely,10 ml of the 100 ppm dye solution was quantified and further diluted to a total volume of 100 ml with distilled water, creating a 10 ppm dye solution. To study adsorption, 50 mg of each of the synthesized nanocomposites was meticulously weighed and introduced into 50 ml of the prepared 10 ppm dye solution. The solution was left to react for a period of 45 minutes in total to test the efficiency of nanocomposite dyes in dye removal.
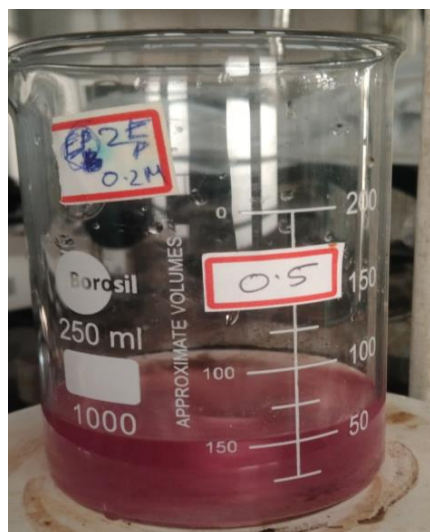
Fig.3.7 Dye nanocomposite interaction

Fig.3.8 Sample for UV analysis

Monitoring of the process of adsorption was conducted via analysis of dye solution samples utilizing UV-visible spectrophotometry every 15-minute interval. This spectroscopic study assisted in the determination of the reduction in dye concentration with time, thus evaluating the adsorption capacity and efficiency of the nanocomposites in the removal of the dye from the solution.

Chapter 4

Results and discussion

4.1 FT-IR SPECTROSCOPY ANALYSIS

The FT-IR spectrum of the pure Na^+-MMT, Starch-MMT Clay, and Chitosan Starch-MMT nanocomposite at various ratios were analysed. The FT-IR absorption bands were confirmed in every instance by analyzing the characteristic bands.

4.1.1 FT-IR spectrum of pure Na^+-MMT clay

The FT-IR spectrum of the Pure Na^+-MMT clay is shown in Fig. 4.1.

For pure Na^+-MMT clay, a broad band at 3455.11cm^{-1} indicates the -OH stretching of water molecules in the interlayer of the clay. The band at 3629.21cm^{-1} represents the -OH stretching of the Al-OH bond. The band observed at 1637.36cm^{-1} corresponds to the -OH bending vibration of water molecules in the interlayer of the clay. The band identified at 1046.16cm^{-1} represents the Si-O-Si stretching vibration and the bands at 524.22cm^{-1} & 463.92cm^{-1} are identified as the Al-O-Si and Si-O-Si bending vibrations respectively. The band observed at 916.01cm^{-1} which belongs to the bending vibration of Al-OH.
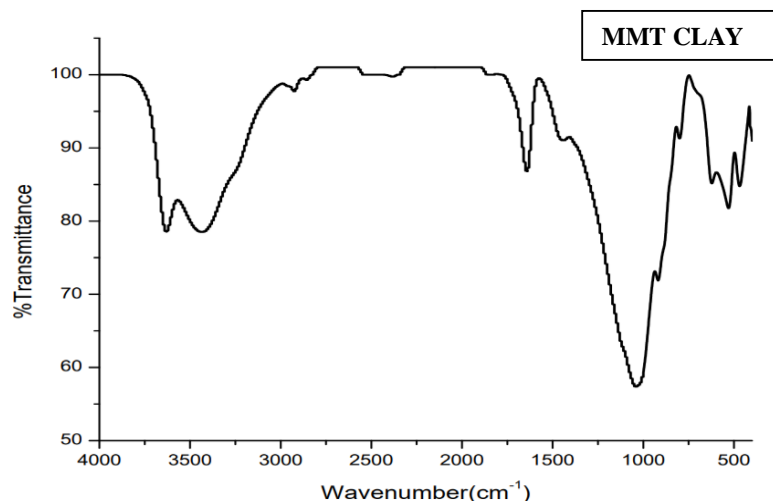
Fig.4.1 FT-IR of Pure Na$^+$-MMT Clay

The vibrational frequencies of the peaks are listed in below table 4.1.

Wavenumber(cm^{-1})	Vibration
3629.21	-OH stretching for Al-OH
3455.11	-OH stretching of water
1637.36	-OH bending of water
1046.16	Si-O-Si stretching
916.01	Al-OH bending
524.22	Al-O-Si bending
463.92	Si-O-Si bending

Table 4.1 Vibrational frequencies of Pure Na$^+$-MMT clay

4.1.2 FT-IR spectrum of Starch-MMT

The FT-IR spectrum of starch-MMT clay is shown in Fig. 4.2.

The bands in the pure Na^+-MMT clay were also observed in the Starch-MMT Clay. In this study, FT-IR analysis was applied to examine the possible interactions between the components of the Starch-MMT nano-composite. The characteristic peak from $3628.81cm^{-1}$ to $3446.97cm^{-1}$ indicates the interaction between starch and MMT. In the spectrum of pure starch, the main characteristic peaks were due to the stretching and bending vibration of hydrogen bonding of the OH group at $3419cm^{-1}$ and $1652cm^{-1}$ respectively. The stretching vibrations of C-O bonding in the C-O-H and C-O-C group in the anhydrous glucose ring appeared at $1163\ cm^{-1}$, $1084cm^{-1}$, and $988\ cm^{-1}$. The characteristic peak of C-O-C ring vibration in starch was located at $765\ cm^{-1}$. Here, $3446.97cm^{-1}$ was due to stretching, $1652cm^{-1}$ was due to the bending of hydrogen bonding of the OH group in the C-OH and C-O-C group in the anhydrous glucose ring. The peak corresponds to $2921.85cm^{-1}$ representing CH_2 stretching. The absorption at $1457.79cm^{-1}$ corresponds to CH bending in alkanes. The additional bands at $3649cm^{-1}$, $3750cm^{-1}$, and $3853cm^{-1}$ represent the OH stretching of alcohol. The broader peak of OH stretching of water around $3628.81cm^{-1}$ in pure MMT becomes less broad in Starch-MMT indicating the replacement of free water in the interlayer of MMT by Starch during the process.
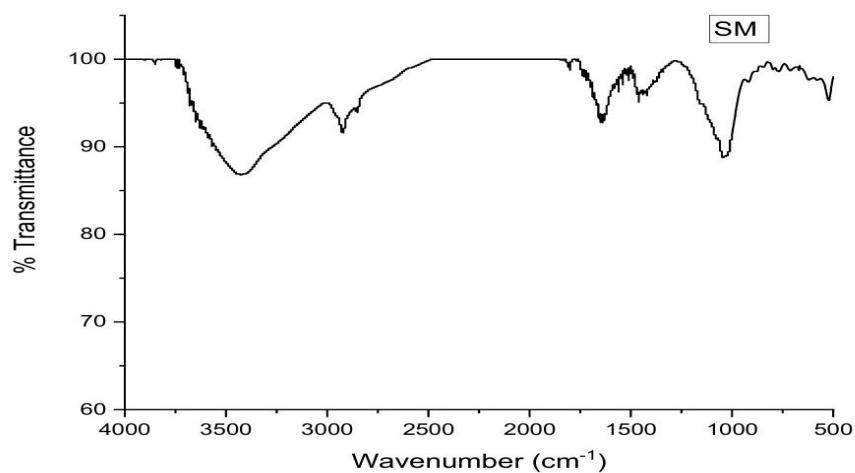
Fig.4.2 FT-IR of Starch-MMT Clay

The vibrational frequencies of the peaks are listed in the below table 4.2

Wavenumber(cm^{-1})	Vibrations
3853.31-3649.16	-OH Stretching vibrations
3628.81	-OH stretching for Al-OH
3446.97	- OH stretching for water
2921.85	-CH$_2$ stretching
1653.39	-OH bending of water
1457.59	-CH bending in alkanes
1045.06	Si-O-Si stretching
519.63	Al-O-Si bending
465.85	Si-O-SI bending

Table 4.2 Vibrational frequencies of Starch-MMT clay

53

4.1.3 FT-IR spectrum of Chitosan Starch MMT 1: 0.1

The FT-IR spectrum of Chitosan St-MMT 1: 0.1 is shown in Fig. 4.3.

The bands in the pure Na^+-MMT clay were also observed in the Starch-MMT Clay. The FT-IR spectrum of chitosan Starch MMT showed a major peak at $2851.79 cm^{-1}$ which signifies the NH group symmetric vibration. There are smaller bands at $1653.6 cm^{-1}$ which indicates the presence of a medium OH bending vibration of water. A peak at $2922.18 cm^{-1}$ indicates the CH vibrations which are characteristic of any organic macromolecule. The presence of peaks near $2851.79 cm^{-1}$ up to $2922.18 cm^{-1}$ signifying the presence of NH (amine salt) stretching along with the presence of a peak at $1653.69 cm^{-1}$ is due to OH bending of water. The characteristic peaks at $468.04 cm^{-1}$, $824.64 cm^{-1}$ represent Si-O-Si and C=C bending vibrations. The absorption at $1019.24 cm^{-1}$ corresponds to C-N stretching in amines and $1458.02 cm^{-1}$ corresponds to CH bending in alkanes. The band at $3447.32 cm^{-1}$ represents the OH stretching of water. The additional bands at $3649.59 cm^{-1}$, $3675 cm^{-1}$, $3821.16 cm^{-1}$, and $3853.65 cm^{-1}$ represent OH stretching of alcohol. No new peaks formed in the composite which means that there has not been any chemical reaction between Starch-MMT and Chitosan. Similar peaks were obtained in the same range of wavenumbers, Validating the incorporation of MMT in the Chitosan matrix.
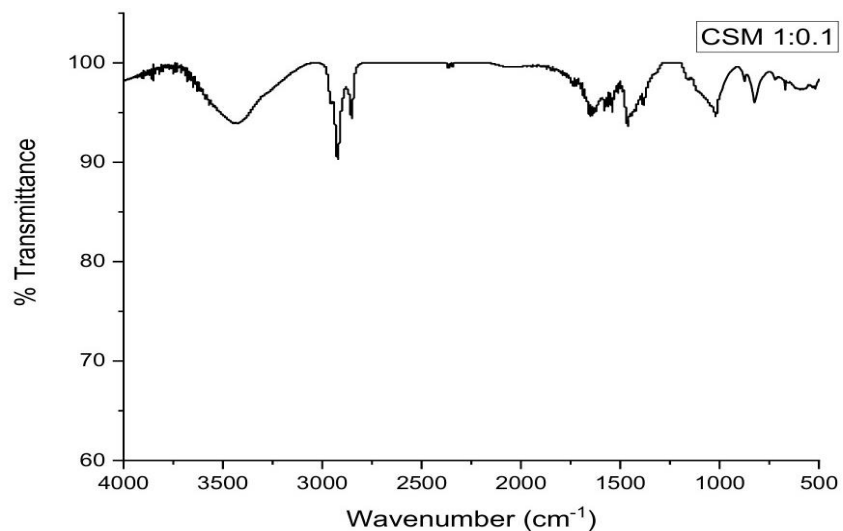
Fig.4.3 FT-IR of Chitosan Starch-MMT 1:0.1

The vibrational frequencies of the peaks are listed in the below table 4.3

Wavenumbers(cm^{-1})	Vibrations
3853.65-3649.59	-OH Stretching vibrations
3447.32	-OH Stretch of H_2O
2922.18	-CH$_2$ Stretching
2851.79	-NH Symmetric vibration
1653.6	-OH Bending of water
1576.7	C=C Stretching in alkenes
1540.95	-NH$_2$ Stretching vibrations
1458.02	-CH Bending in alkane
1019.24	C-N Stretching in amino
824.64	C=C Bending in alkenes
468.04	Si-O-Si Bending

Table 4.3 Vibrational frequencies of Chitosan St-MMT 1: 0.1

4.1.4 FT-IR spectrum of Chitosan Starch MMT 1: 0.5

The FT-IR spectrum of Chitosan St-MMT 1: 0.5 is shown in Fig. 4.4.

The bands in the pure Na^+-MMT clay were also observed in the Starch-MMT Clay. The FT-IR spectrum of Chitosan Starch-MMT showed a major peak at 2851.60cm^{-1} which signifies the NH group symmetric vibration. There are smaller bands at 1653.71cm^{-1} which indicates the presence of a medium OH bending Vibration of water. A peak at 2922cm^{-1} indicates the CH vibrations which are characteristic of any organic macromolecule. The presence of peaks near 2851.60cm^{-1} up to 2922cm^{-1} signifying the presence of NH (amine salt) stretching along with the presence of a peak at 1653.71cm^{-1} is due to OH bending of water. The characteristic peaks at 464.45cm^{-1}, 521.27cm^{-1} represent Si-O-Si and Al-O-Si bending vibrations. The absorption at 1019.40cm^{-1} corresponds to C-N stretching in amines and 1458.06cm^{-1} corresponds to CH bending in alkanes. The band at 3447.30cm^{-1} represents the OH stretching of water. The additional bands at 3853.65cm^{-1} represent the OH stretching of alcohol. No new peaks formed in the composite which means that there has not been any chemical reaction between Starch-MMT and Chitosan. Similar peaks were obtained in the same range of wavenumbers, Validating the incorporation of MMT in the Chitosan matrix.
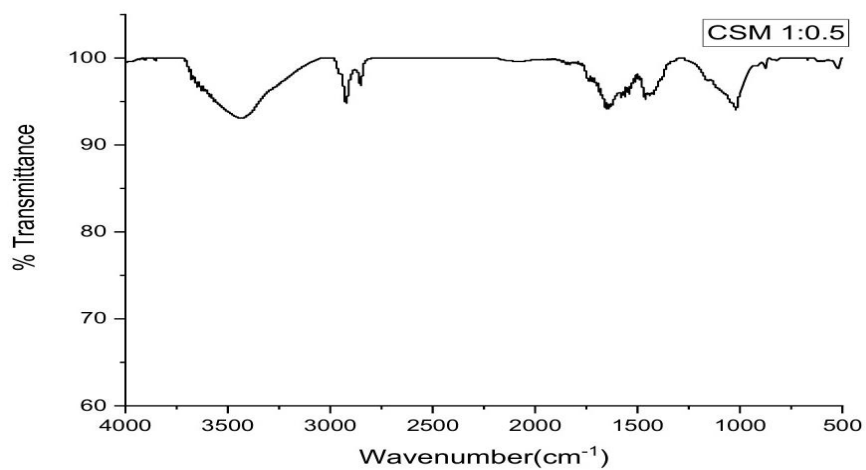
Fig.4.4 FT-IR of Chitosan Starch-MMT 1:0.5

The vibrational frequencies of the peaks are listed in the below table 4.4

Wavenumbers(cm^{-1})	Vibrations
3853.65	-OH Stretching vibrations
3447.30	-OH Stretch of H_2O
2922	-CH$_2$ Stretching
2851.60	-NH Symmetric vibration
1653.71	-OH Bending of water
1458.06	-CH Bending in alkane
1019.40	C-N Stretching in amino
521.27	Al-O-Si Bending
464.45	Si-O-Si Bending

Table 4.4 Vibrational frequencies of Chitosan St-MMT 1: 0.5

57

4.1.5 FT-IR spectrum of Chitosan Starch MMT 1: 1

The FT-IR spectrum of Chitosan St-MMT 1: 1 is shown in Fig. 4.5.

The bands in the pure Na^+-MMT clay were also observed in the Starch-MMT Clay. The FT-IR spectrum of Chitosan Starch MMT showed a major peak at 2851.60cm^{-1} which signifies the NH group symmetric vibration. There are smaller bands at 1653.66cm^{-1} which indicates the presence of a medium OH bending Vibration of water. A peak at 2921.39cm^{-1} indicates the CH vibrations which are characteristic of any organic macromolecule. The presence of peaks near 2851.60cm^{-1} up to 2921.39cm^{-1} signifying the presence of NH (amine salt) stretching along with the presence of a peak at 1653.66cm^{-1} is due to OH bending of water. The characteristic peaks at 464.72cm^{-1} represent Si-O-Si bending vibrations. The absorption at 1020.01cm^{-1} corresponds to C-N stretching in amines and 1458.12cm^{-1} corresponds to CH bending in alkanes. The band at 3447.14cm^{-1} represents the OH stretching of water. No new peaks formed in the composite which means that there has not been any chemical reaction between Starch-MMT and Chitosan. Similar peaks were obtained in the same range of wavenumbers, Validating the incorporation of MMT in the Chitosan matrix.
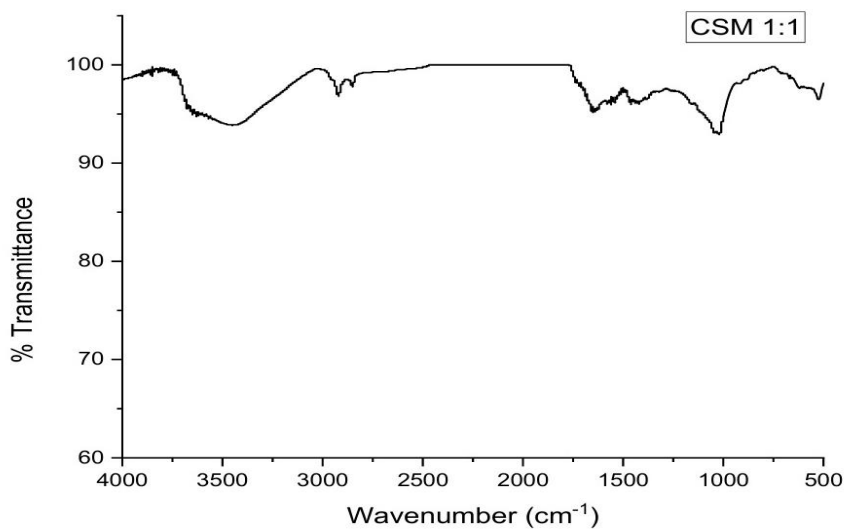
Fig.4.5 FT-IR of Chitosan Starch-MMT 1:1

The vibrational frequencies of the peaks are listed in the below table 4.5

Wavenumbers(cm⁻¹)	Vibrations
3447.14	-OH Stretch of H_2O
2921.39	-CH$_2$ Stretching
2851.6	-NH Symmetric vibration
1653.66	-OH Bending of water
1458.12	-CH Bending in alkane
1020.01	C-N Stretching in amino
521.27	Al-O-Si Bending
464.72	Si-O-Si Bending

Table 4.5 Vibrational frequencies of Chitosan St-MMT 1: 1

4.2 XRD ANALYSIS

The degree of intercalation/exfoliation can be determined by observing the position, shape and intensity of the XRD peak for Chitosan Starch-MMT clay nanocomposites. We observed the change in (001) reflection peak in each graph. The d-spacing were calculated by considering the (001) reflection(67).
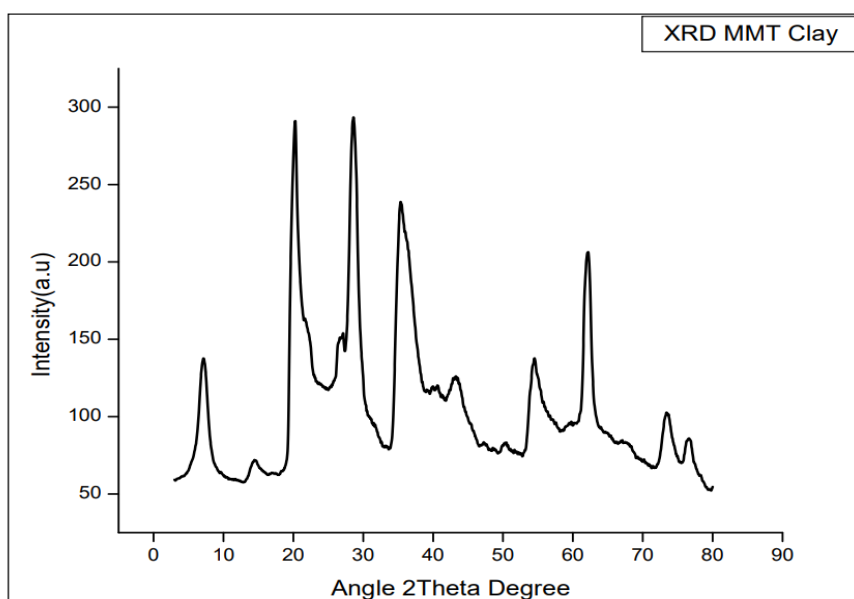
4.2.1 XRD analysis of Pure Na⁺-MMT clay

Fig.4.6 XRD of Pure Na⁺-MMT clay

Sample	Angle 2θ(degree)	d–spacing (A°)
Pure Na⁺-MMT clay	7.081	12.47

Table 4.6 d-spacing of Pure Na⁺-MMT clay

4.2.2 XRD of St-MMT Clay
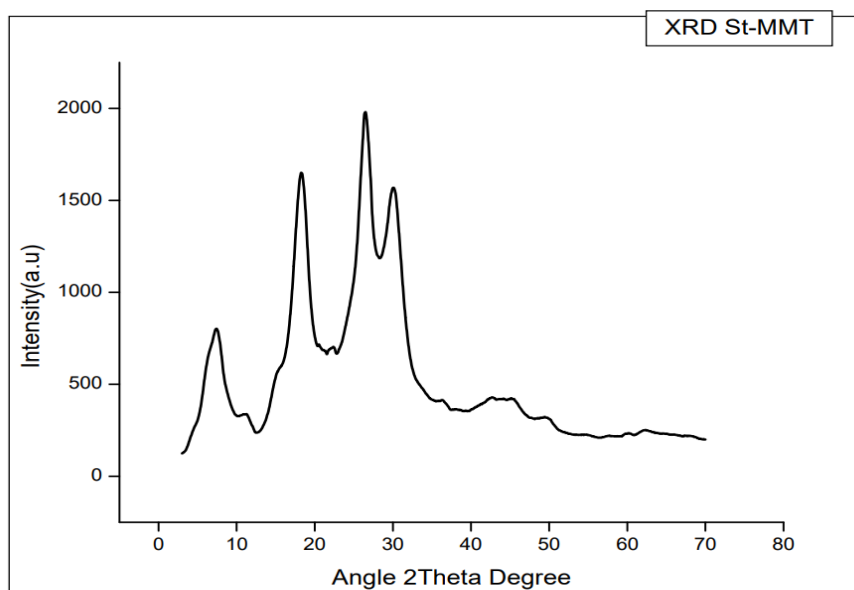
Fig.4.7 XRD of Starch-MMT clay

Sample	Angle 2θ (degree)	d–spacing (A°)
Starch-MMT clay	7.160	12.34

Table 4.7 d-spacing of Starch-MMT clay

61

4.2.3 XRD OF Chitosan St-MMT 1: 0.1
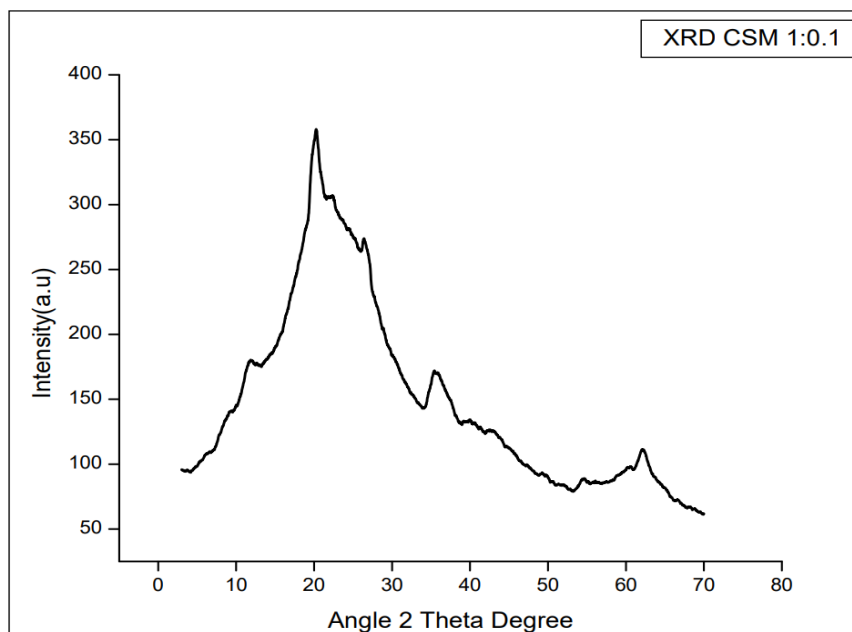
Fig.4.8 XRD of Chitosan Starch-MMT clay 1:0.1

Sample	Angle 2θ (degree)	d–spacing (A°)
Chitosan St-MMT 1:0.1	7.068	12.49

Table 4.8 d-spacing of Chitosan Starch-MMT clay 1:0.1

4.2.4 XRD OF Chitosan St-MMT 1: 0.5

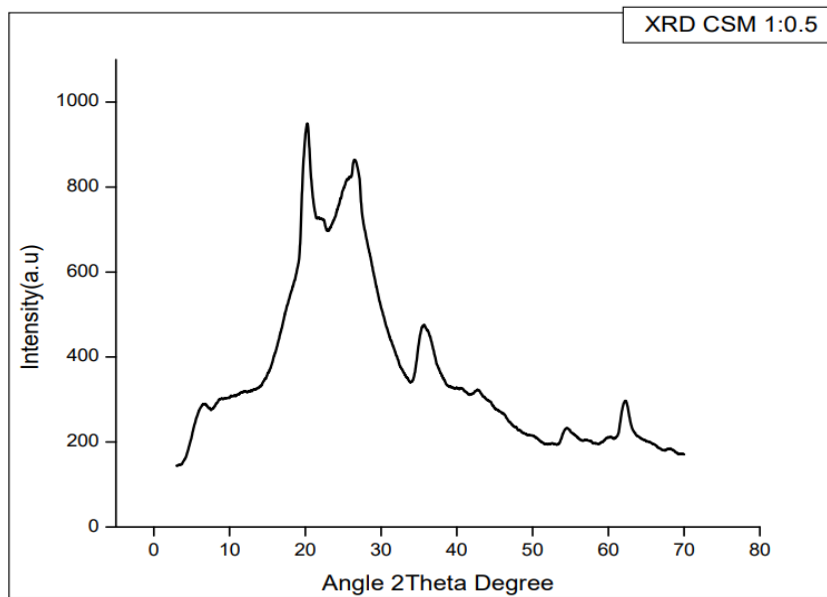
Fig.4.9 XRD of Chitosan Starch-MMT clay 1:0.5

Sample	Angle 2θ (degree)	d–spacing (A°)
Chitosan St-MMT 1:0.5	6.540	13.49

Table 4.9 d-spacing of Chitosan Starch-MMT clay 1:0.5

4.2.5 XRD OF Chitosan St-MMT 1: 1
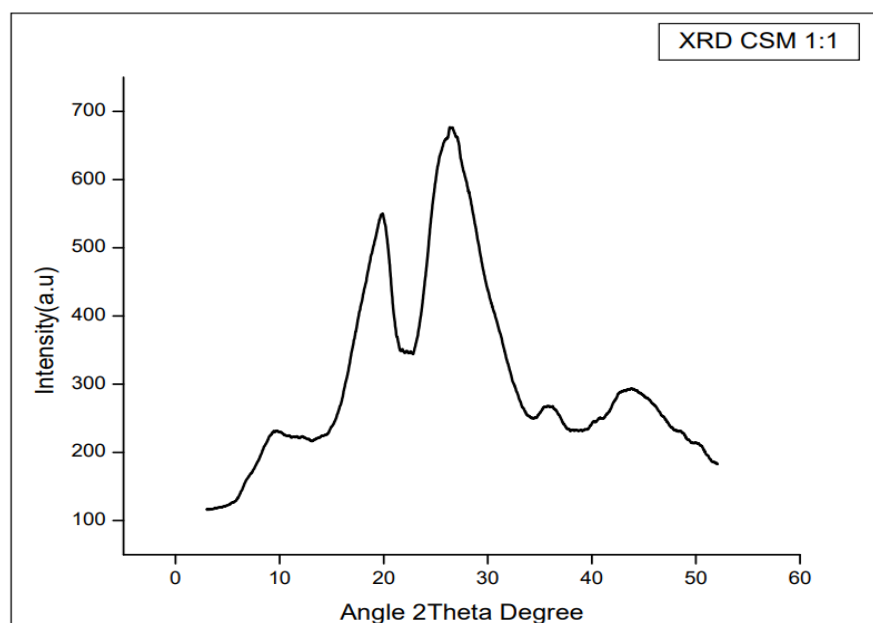
Fig.4.10 XRD of Chitosan Starch-MMT clay 1:1

Sample	Angle 2θ (degree)	d–spacing (A°)
Chitosan St-MMT 1:1	5.562	15.88

Table 4.10 d-spacing of Chitosan Starch-MMT clay 1:1

On comparing all the (001) reflection peak of the pure Clay, Starch-MMT and Chitosan-Starch MMT clay is listed in the table.4.11.

Sample	Angle 2θ (degree)	d–spacing (A°)
Pure Na⁺-MMT clay	7.081	12.47
Starch-MMT clay	7.160	12.34
Chitosan Starch-MMT 1:0.1	7.068	12.49
Chitosan Starch-MMT 1:0.5	6.540	13.49
Chitosan Starch-MMT 1:1	5.562	15.88

Table 4.11 Comparison of d-spacing of pure Clay, Starch-MMT, and Chitosan-Starch MMT

X-ray diffraction is the commonly used technique to calculate the d-spacing of nano clay (68). The d-spacing is calculated using the diffraction peaks in the XRD patterns which is given by Bragg's equation $\lambda = 2d\sin\theta$ where λ is the wavelength, d corresponds to interplanar spacing and θ is the position of diffraction. During incorporation of nano clay into the matrix, the polymer will force the platelets apart causing the diffraction peaks to shift to a lower angle.

Table.4.11. displays the XRD patterns of pure Na⁺-MMT clay, starch MMT, and Chitosan Starch MMT nanocomposite in different ratios. Here, by comparison with MMT clay, the Chitosan Starch MMT 1:1 d-spacing increases from 12.47 A° to 15.88A°.

From the data, in comparison to the d-spacing of pure Na⁺ -MMT clay, the starch MMT clay d-spacing values decrease. It can be inferred that the decrease in d-spacing was observed due to agglomeration of MMT as the

65

concentration of nano clay was increased (31). As the composition of chitosan-starch-MMT nanocomposite increases from 1:0.1 to 1:0.5 and 1:1, the d-spacing value progressively expands, indicating enhanced interlayer spacing.

4.3 THERMOGRAVIMETRIC ANALYSIS (TGA)

Thermogravimetric analysis (TGA) analysis was performed to determine the thermal stability of the materials. It shows the TGA curves of pure materials (St and MMT) as well as nanocomposites (St-MMT and St-MMT/Chitosan)(9).
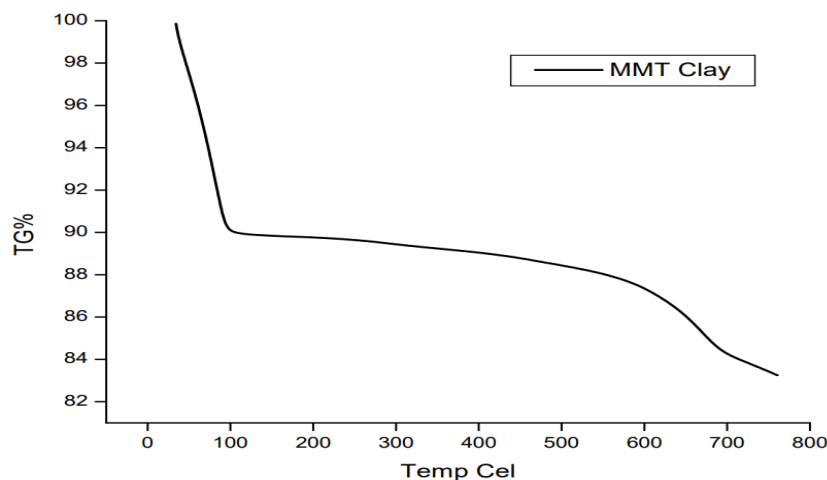
4.3.1 TGA of pure Na^+-MMT clay

Fig.4.11 TGA of Pure Na^+-MMT clay

Sample	T(^{0}C)	Weight loss (%)
Pure Na^+-MMT Clay	98.2	90.2

Table 4.12 Thermal degradation of Pure Na^+-MMT clay

66

4.3.2 TGA of St-MMT clay
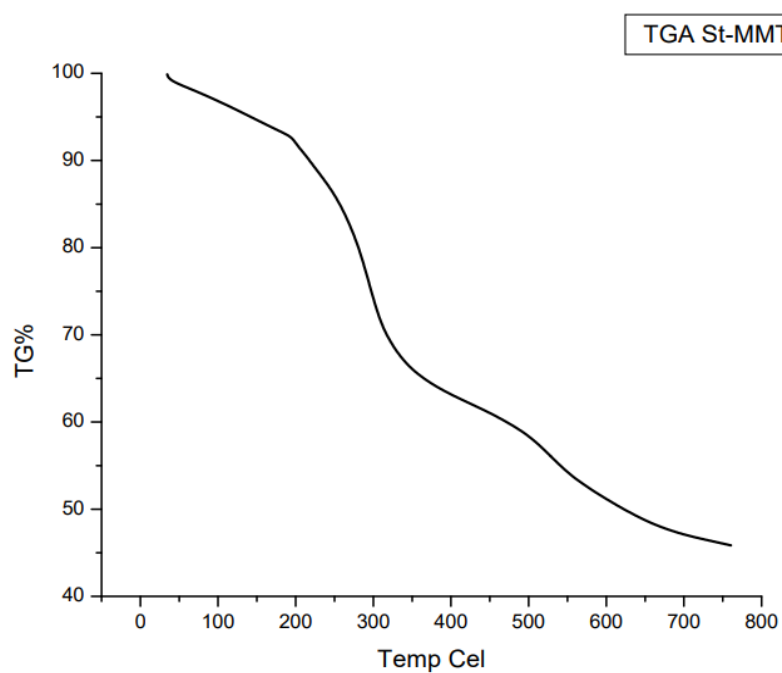
Fig.4.12 TGA of Starch-MMT clay

Sample	T(^{0}C)	Weight loss (%)
St-MMT Clay	245.6	90.5

Table 4.13 Thermal degradation of Starch-MMT clay

67

4.3.3 TGA of Chitosan St-MMT 1:0.1
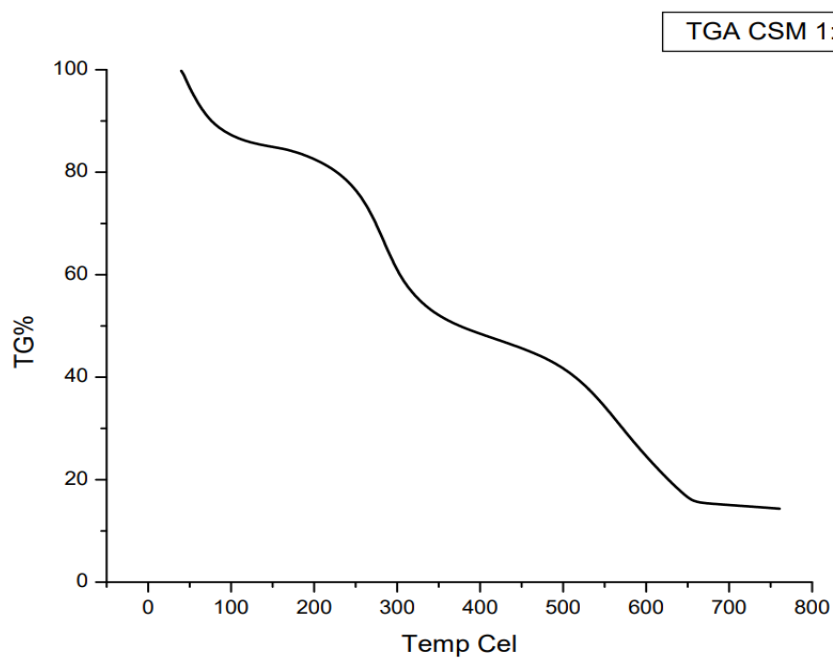
Fig.4.13 TGA of Chitosan Starch-MMT clay 1:0.1

Sample	T(^{0}C)	Weight loss (%)
Chitosan St-MMT 1:0.1	244.5	80.1

Table 4.14 Thermal degradation of Chitosan Starch-MMT clay 1:0.1

4.3.4 TGA of Chitosan St-MMT 1:0.5
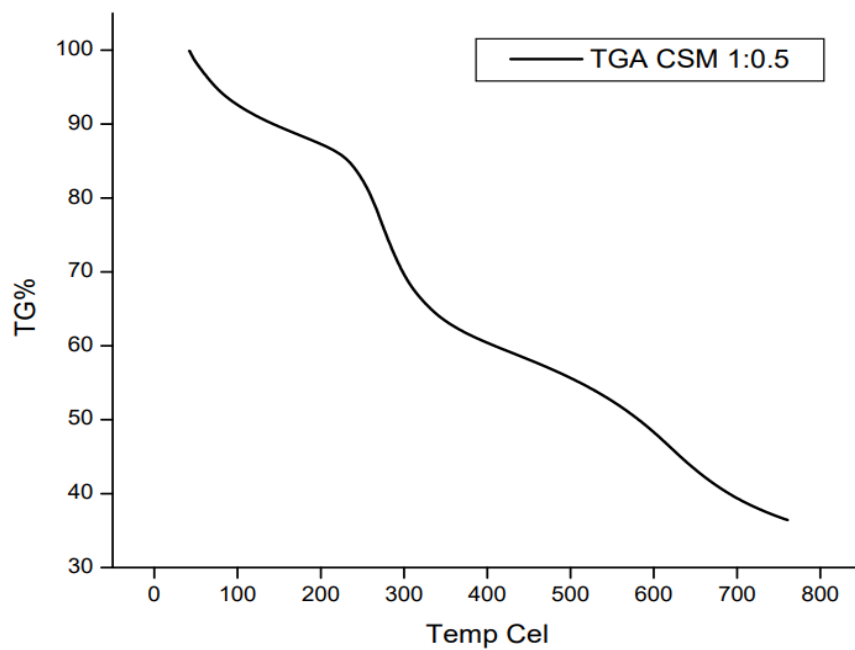
Fig.4.14 TGA of Chitosan Starch-MMT clay 1:0.5

Sample	T(^{0}C)	Weight loss (%)
Chitosan St-MMT 1:0.5	244.2	85.5

Table 4.15: Thermal degradation Chitosan Starch-MMT clay 1:0.5

4.3.5 TGA of Chitosan St-MMT 1:1

Fig.4.15 TGA of Chitosan Starch-MMT clay 1:1

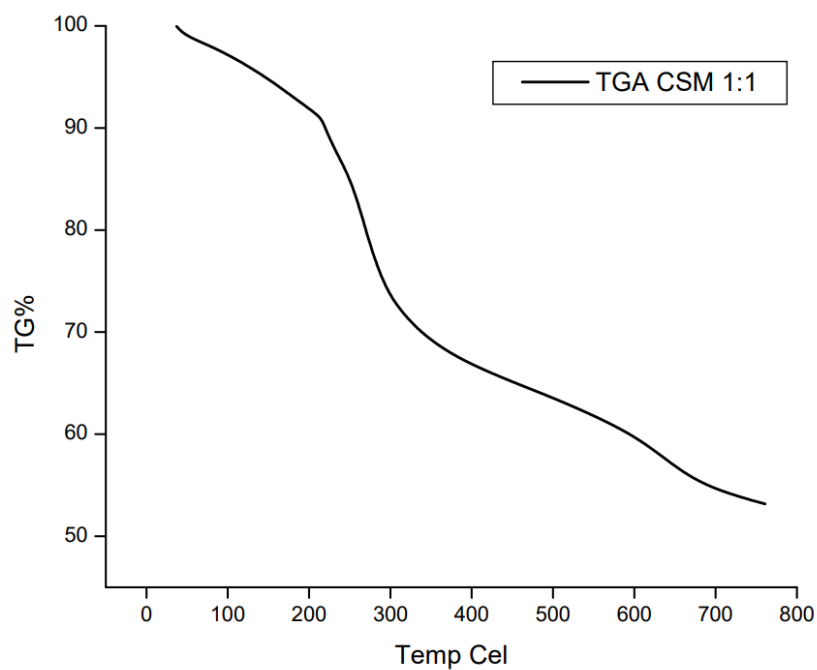| Sample	T(^{0}C)	Weight loss (%)
Chitosan St-MMT 1:1	226.9	90.3

Table 4.16: Thermal degradation of Chitosan Starch-MMT clay 1:1

In comparison of TGA Data obtained for pure Clay, Starch-MMT, and Chitosan-Starch MMT clay is listed in Table 4.17

Sample	T(^{o}C)	Weight loss (%)
pure Na$^+$-MMT clay	98.2	90.2
Starch-MMT clay	245.6	90.5
Chitosan St-MMT 1:0.1	244.5	80.1
Chitosan St-MMT 1:0.5	244.2	85.5
Chitosan St-MMT 1:1	226.9	90.3

Table 4.17 Comparison of the thermal degradation of various nanocomposites

The starch MMT clay and chitosan starch MMT in various ratios were compared to the TGA data analysis of pure Na$^+$-MMT clay. Because of the water loss from the samples, each sample showed the first degradation stage at around 100°C. Because starch's hydroxyl groups form hydrogen bonds, it absorbs a lot of water and environmental moisture. The greatest level of starch decomposition (240°C) was matched by the second degradation step. This stage involved the removal of poly-hydroxylic groups, as well as the breakdown and depolymerization of the chains(69).

At 98°C, MMT displayed a single deterioration stage that was caused by water loss. The absence of clay dehydroxylation in the MMT curve suggested that MMT had excellent thermal stability within the temperature range under study. Nano clay marginally increased the starch's thermal

71

stability in the St-MMT nanocomposite to roughly 245.6°C. This enhancement might result from the nano clay's ability to block the volatile substances produced during the polymer's breakdown (70). Furthermore, MMT's intercalated structure may stop water from migrating and evaporating. Additionally, MMT protected the starch's exposed hydroxyl groups, which slowed the polysaccharide's heat depolymerization.

Furthermore, because of their configuration properties, inorganic materials exhibited superior thermal stability when compared to biological materials. Consequently, the thermal stability of organic polymer materials would be significantly increased by the addition of inorganic particles (71). The breakdown of the starch sub-products produced during the starch degradation process was the subject of the following processes. The polymerization of chitosan on the surface of the St-MMT nanocomposite causes the thermal degradation to decrease in the case of St-MMT/Chitosan nanocomposite of different ratios of 1:0.1, 1:0.5, and 1:1 (244.5°C, 244.2°C and 226.9°C). The barrier properties of nano clay were not observed, and the compound's decomposition temperature was shifted to lower temperatures (215°C).

4.4 EVALUATION OF DYE ADSORPTION EFFICIENCY

To assess the performance of the prepared nanocomposite in various ratios in eliminating dye contaminants from a solution, an adsorption efficiency test is performed. The process starts with the preparation of a 10 ppm dye solution, which is used as the model contaminant. The prepared nanocomposite is subsequently introduced into the dye solution, mixed well, and left to incubate for 45 minutes, allowing the nanocomposite to interact with the dye molecules. The adsorption capacity of the nanocomposite is determined via a UV-visible

spectrometer with readings every 15 minutes to track the reduction in the concentration of the dye over time. Through a determination of the absorbance value recorded by the spectrometer, the percentage of dye removal can be computed, showing the adsorption capacity of the nanocomposite and revealing its future use in wastewater treatment and environmental cleanup.

4.4.1 UV-Vis Spectrum Analysis of Dye Solution
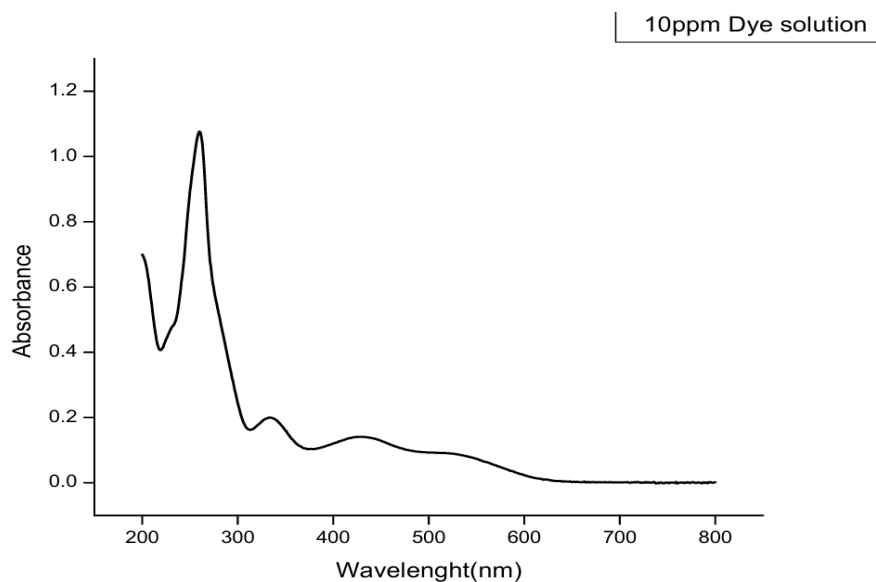
Fig.4.16 UV-Visible spectrum of Dye Solution

Sample	Wavelength(nm)	Absorbance
Alizarin Red Dye	260	1.0764

Table 4.18 UV-Visible Analysis of Alizarin Red Dye Solution

73

4.4.2 UV-Vis Spectrum Analysis of Dye Solution Treated with Starch-MMT
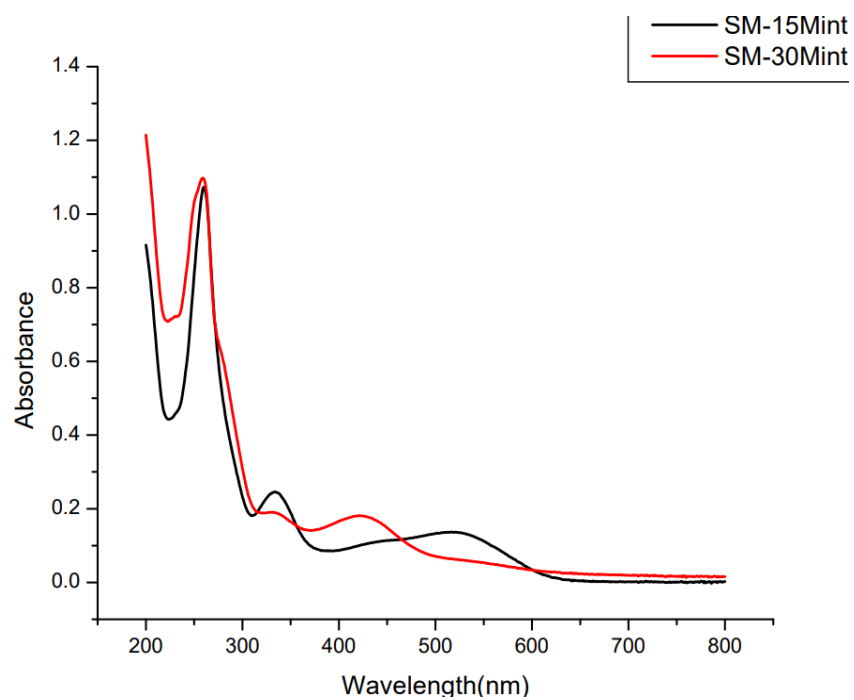
Fig.4.17 UV-Visible spectrum of Dye solution in Starch-MMT

Sample	Wavelength(nm)	Absorbance
Starch-MMT clay	260	1.0966

Table 4.19 UV-Visible Analysis of dye solution in Starch-MMT Clay

4.4.3 UV-Vis Spectrum Analysis of Dye Solution Treated with Chitosan Starch MMT 1:0.1
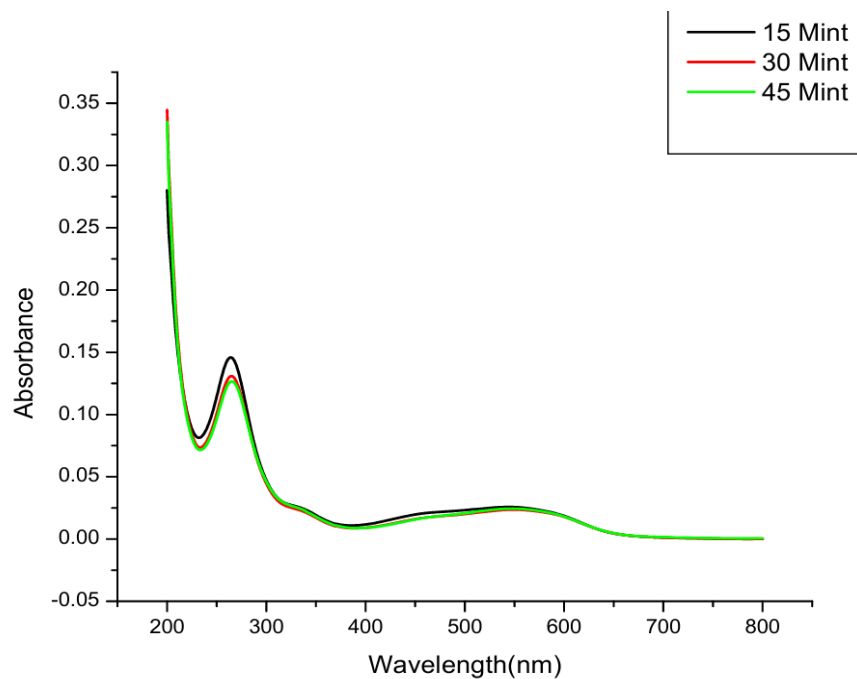
Fig.4.18 UV-Visible spectrum of Dye solution in 1:0.1 Chitosan-Starch-MMT Nanocomposite

Sample	Wavelength(nm)	Absorbance
Chitosan St-MMT 1:0.1	260	0.2923

Table 4.20 UV-Visible Analysis of Dye solution in Chitosan St-MMT in the ratio of 1:0.1

4.4.4 UV-Vis Spectrum Analysis of Dye Solution Treated with Chitosan Starch MMT 1:0.5
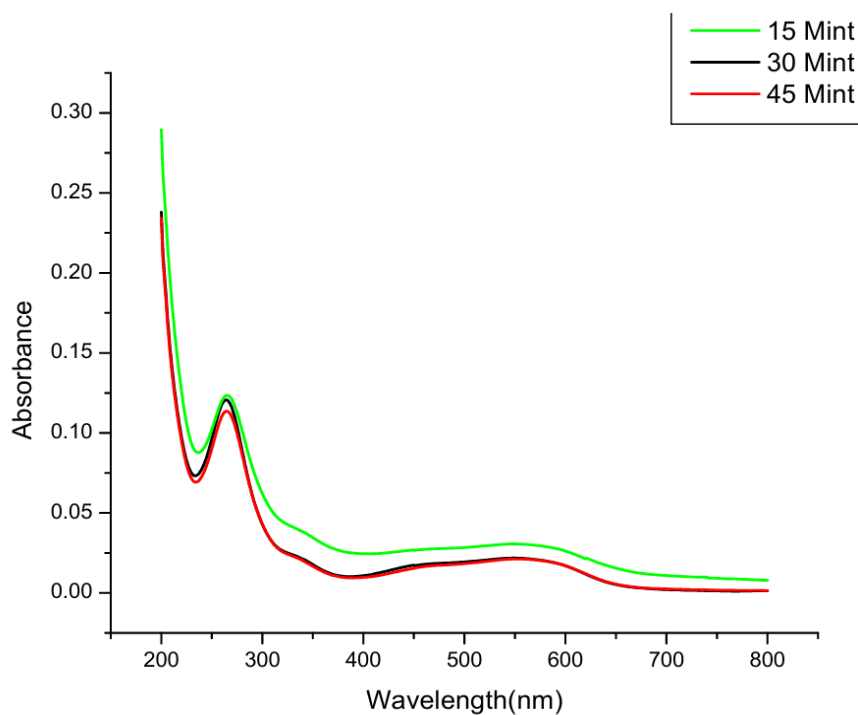
Fig.4.19: UV-visible spectrum of Dye solution in 1:0.5 Chitosan-Starch-MMT Nanocomposite

Sample	Wavelength(nm)	Absorbance
Chitosan St-MMT 1:0.5	260	0.1218

Table 4.21 UV-Visible Analysis of Dye Solution in Chitosan St-MMT in the ratio of 1:0.5

4.4.5 UV-Vis Spectrum Analysis of Dye Solution Treated with Chitosan Starch MMT 1:1

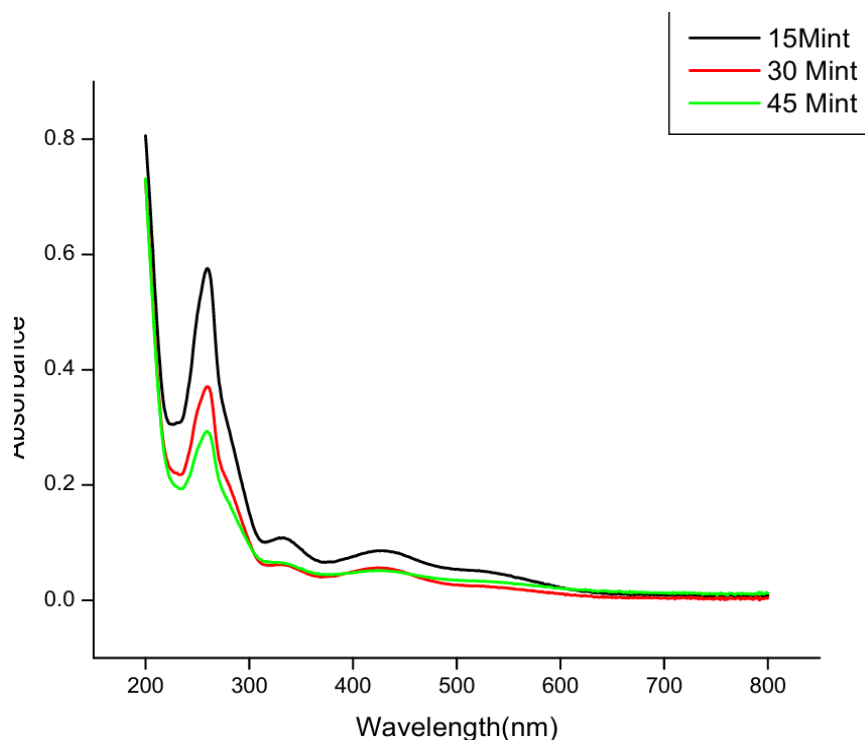**Fig.4.20 UV-Visible spectrum of Dye solution in 1:1 Chitosan-Starch-MMT Nanocomposite**

Sample	Wavelength(nm)	Absorbance
Chitosan St-MMT 1:1	260	0.1104

Table 4.22 UV-Visible Analysis of Dye solution in Chitosan St-MMT in the ratio of 1:1

In a comparison of UV Data obtained for Dye, Starch-MMT, and Chitosan-Starch MMT clay in different ratios is listed in table 4.23

Sample	Wavelength (nm)	Absorbance
Alizarin Red Dye	260	1.0764
Starch-MMT clay	260	1.0966
Chitosan St-MMT 1:0.1	260	0.2923
Chitosan St-MMT 1:0.5	260	0.1218
Chitosan St-MMT 1:1	260	0.1104

Table 4.23 Comparison of UV Data of Various Nanocomposite

The absorption efficiency of different Chitosan-Starch-MMT (CSM) nanocomposites with the dye was assessed using their absorbance at 260nm wavelength. The UV analysis data strongly confirms the high efficiency of our prepared chitosan-starch-MMT nanocomposites in adsorbing alizarin red dye. The absorbance of the pure dye solution is 1.076 Abs, while the starch-MMT clay alone shows a slightly higher absorbance of 1.096 Abs, indicating minimal dye removal. However, when using the chitosan-starch-MMT nanocomposites, a significant reduction in absorbance is observed with the CSM nanocomposites: 0.2923 for CSM (1:0.1), 0.1218 for CSM (1:0.5), and 0.1104 for CSM (1:1). This remarkable adsorption performance can be attributed to the increase in d-spacing within the CSM nanocomposites, which enhances the available surface area and interlayer accessibility, facilitating greater dye molecule adsorption. It was interesting to observe that the

CSM 1:1 ratio had tremendous variation in the values of absorbance over the 15-minute time period, which indicated that, the time contact with nanocomposites increases absorbance decreases.

The structural characteristics of the nanocomposites are responsible for the observed variation in the efficiency of absorption. Among the CSM nanocomposites, the 1:1 composition exhibits the highest d-spacing, making it a more intercalated nanocomposite. This enhanced intercalation improves adsorption efficiency by providing greater surface area, increased porosity, and improved interaction sites for dye molecules, all of which are characteristic properties of intercalated nanocomposites.

Chapter 5

Conclusions

Starch-montmorillonite and chitosan-starch-montmorillonite (CS-MMT) nanocomposites were successfully synthesized and thoroughly characterized, showcasing their promising capability to remove reactive dyes from wastewater effectively. The synthesis process involved preparing separate solutions of starch and Na^+-MMT, followed by ultrasonic treatment. These solutions were then combined under controlled temperature conditions to create a Starch-MMT nanocomposite. After this, chitosan was incorporated into the nanocomposite, resulting in a Chitosan-Starch-montmorillonite nanocomposite that enhanced the material's adsorption properties. Structural, thermal, and adsorption studies were conducted to understand the interactions within the nanocomposites and evaluate their efficiency in dye removal.

Fourier-transform infrared (FT-IR) spectroscopy demonstrated significant interactions among the components of the composite. Characteristic peaks associated with the functional groups of montmorillonites (MMT), chitosan, and starch were identified. Hydroxyl (-OH) and amine (NH) stretching bands confirmed that the components were physically incorporated. The absence of new peaks indicated that no chemical reactions took place, thereby preserving the structural integrity of the nanocomposite.

X-ray diffraction studies showed evidence of MMT intercalation within the polymer matrix. An increase in d-spacing was observed for the CS-MMT nanocomposite with a 1:1 ratio, confirming that the polymer chains effectively incorporated between the clay layers. The decrease in d-spacing of starch-MMT clay due to MMT agglomeration is subsequently counteracted by the progressive expansion of d-spacing in chitosan-starch-MMT nanocomposites, indicating enhanced interlayer spacing.

Thermogravimetric analysis (TGA) was conducted to evaluate the degradation behavior of the composites. The results indicated that montmorillonite (MMT) enhanced the thermal stability of starch by increasing its decomposition temperature. MMT served as a thermal barrier, which reduced the volatility of degradation products and slowed down the depolymerization of starch's hydroxyl groups. However, chitosan altered the degradation pathway, resulting in decreased thermal stability of the chitosan-MMT (CS-MMT) nanocomposites, particularly at higher concentrations of chitosan, where the protective barrier effect of MMT was diminished.

The absorption efficiency of the CS-MMT nanocomposites was evaluated using UV-Vis spectroscopy at a wavelength of 260 nm. The results confirm the exceptional adsorption efficiency of the Chitosan-Starch-MMT (CSM) nanocomposites in removing alizarin red dye from aqueous solutions. The pure dye solution exhibited an absorbance of 1.076 Abs, while the starch-MMT clay alone showed a slightly higher absorbance of 1.096 Abs, indicating minimal adsorption. However, the CSM nanocomposites demonstrated a significant reduction in absorbance, with values of 0.2923 Abs for CSM (1:0.1), 0.1218 Abs for CSM (1:0.5), and

0.1104 Abs for CSM (1:1). This highlights the effectiveness of these nanocomposites in dye removal. The improved adsorption efficiency is closely linked to the increase in d-spacing within the nanocomposites, which enhances interlayer accessibility and available surface area for dye adsorption. Among the formulations, the CSM (1:1) nanocomposite exhibits the highest d-spacing, making it a more intercalated structure with enhanced porosity and interaction sites. These structural characteristics contribute to its superior adsorption capability.

The characterization studies confirmed the successful synthesis of CS-MMT nanocomposites, which have potential applications in wastewater treatment. FT-IR and XRD analyses demonstrated the effective incorporation of MMT into the polymer matrix. Additionally, TGA results highlighted MMT's role in enhancing the thermal stability of starch. UV-Vis spectroscopy indicated that the CS-MMT nanocomposite with a 1:1 ratio exhibited the most stable and efficient dye absorption capacity, making it the most suitable candidate for practical applications in dye removal. This study suggests that CS-MMT nanocomposites, particularly in the 1:1 ratio, are promising materials for environmental remediation efforts.

References

1. Sharma P, Nanda K, Yadav M, Shukla A, Srivastava SK, Kumar S, et al. Remediation of noxious wastewater using nanohybrid adsorbent for preventing water pollution. Chemosphere. 2022;292:133380.

2. Pandey S, Ramontja J. PTurning to Nanotechnology for Water Pollution Control: Applications of Nanocomposites. Focus Sci. 2016;2(2):1–10.

3. Liu J, Ma Y, Xu T, Shao G. Preparation of zwitterionic hybrid polymer and its application for the removal of heavy metal ions from water. J Hazard Mater. 2010;178(1):1021–9.

4. Momina, Shahadat M, Isamil S. Regeneration performance of clay-based adsorbents for the removal of industrial dyes: A review. RSC Adv. 2018;8(43):24571–87.

5. Madhumitha G, Fowsiya J, Mohana Roopan S, Thakur VK. Recent advances in starch–clay nanocomposites. Int J Polym Anal Charact. 2018 May;23(4):331–45.

6. Bernkop-Schnürch A, Dünnhaupt S. Chitosan-based drug delivery systems. Eur J Pharm Biopharm. 2012;81(3):463–9.

7. Vakili M, Rafatullah M, Salamatinia B, Abdullah AZ, Ibrahim MH, Tan KB, et al. Application of chitosan and its derivatives as adsorbents for dye removal from water and wastewater: A review. Carbohydr Polym. 2014;113:115–30.

8. Han YS, Lee SH, Choi KH, Park I. Preparation and characterization of chitosan–clay nanocomposites with antimicrobial activity. J Phys Chem Solids. 2010;71(4):464–7.

9. Olad A, Azhar FF. Eco-friendly biopolymer/clay/conducting polymer nanocomposite: Characterization and its application in reactive dye removal. Fibers Polym. 2014;15(6):1321–9.

10. Konta J. Clay science at the threshold of the new millennium: a look at the history and present trends. Acta Univ Carolinae Geol. 2000;44(2–4):11–48.

11. Grim RE. Clay Mineralogy Diagram.Pdf. 1953;

12. Bergaya F, Lagaly G. Chapter 1 General Introduction: Clays, Clay Minerals, and Clay Science. In: Bergaya F, Theng BKG, Lagaly GBTD in CS, editors. Handbook of Clay Science. Elsevier; 2006. p. 1–18.

13. Olad A. Polymer/Clay Nanocomposites. In: Reddy B, editor. Rijeka: IntechOpen; 2011. p. Ch. 7.

14. Chen B, Evans JRG, Greenwell HC, Boulet P, Coveney P V, Bowden AA, et al. A critical appraisal of polymer–clay nanocomposites. Chem Soc Rev. 2008;37(3):568–94.

15. THOMAS ANNT, DAS M, RAMESAN S. EXPLORING THE CONCENTRATION EFFECT OF ACID-AMINE ADDUCT TO THE INTERGALLERY OF Na+ MONTMORILLONITE. St. Teresa's College (Autonomous), Ernakulam; 2019.

16. Tournassat C, Bourg IC, Steefel CI, Bergaya F. Chapter 1 - Surface Properties of Clay Minerals. In: Tournassat C, Steefel CI, Bourg IC, Bergaya FBTD in CS, editors. Natural and Engineered Clay Barriers. Elsevier; 2015. p. 5–31.

17. Guggenheim S, Martin RT. Definition of Clay and Clay Mineral:

Joint Report of the Aipea Nomenclature and CMS Nomenclature Committees. Clays Clay Miner. 2024/02/28. 1995;43(2):255–6.

18. Mittal V. Polymer layered silicate nanocomposites: A review. Materials (Basel). 2009;2(3):992–1057.

19. Kloprogge JT, Komarneni S, Amonette JE. Synthesis of Smectite Clay Minerals: A Critical Review. Clays Clay Miner. 2024/02/28. 1999;47(5):529–54.

20. Jo BW, Park SK, Kim DK. Mechanical properties of nano-MMT reinforced polymer composite and polymer concrete. Constr Build Mater. 2008;22(1):14–20.

21. Bandara WMAT, Krishantha DMM, Perera JSHQ, Rajapakse RMG, Tennakoon DTB. Preparation, Characterization and Conducting Properties of Nanocomposites of Successively Intercalated Polyaniline (PANI) in Montmorillonite (MMT). J Compos Mater. 2005 May;39(9):759–75.

22. Aksu I, Bazilevskaya E, Karpyn ZT. Swelling of clay minerals in unconsolidated porous media and its impact on permeability. GeoResJ. 2015;7:1–13.

23. Chung YL, Ansari S, Estevez L, Hayrapetyan S, Giannelis EP, Lai HM. Preparation and properties of biodegradable starch–clay nanocomposites. Carbohydr Polym. 2010;79(2):391–6.

24. Zhao R, Torley P, Halley PJ. Emerging biodegradable materials: starch- and protein-based bio-nanocomposites. J Mater Sci. 2008;43(9):3058–71.

25. Haroon M, Wang L, Yu H, Abbasi NM, Zain-ul-Abdin, Saleem M, et al. Chemical modification of starch and its application as an adsorbent material. RSC Adv. 2016;6(82):78264–85.

26. Kringel DH, El Halal SLM, Zavareze E da R, Dias ARG. Methods

for the Extraction of Roots, Tubers, Pulses, Pseudocereals, and Other Unconventional Starches Sources: A Review. Starch - Stärke. 2020 Nov;72(11–12):1900234.

27. Fu BX. Asian noodles: History, classification, raw materials, and processing. Food Res Int. 2008;41(9):888–902.

28. Bakshi PS, Selvakumar D, Kadirvelu K, Kumar NS. Comparative study on antimicrobial activity and biocompatibility of N-selective chitosan derivatives. React Funct Polym. 2018;124:149–55.

29. Wang J, Zhuang S. Removal of various pollutants from water and wastewater by modified chitosan adsorbents. Crit Rev Environ Sci Technol. 2017 Dec;47(23):2331–86.

30. Rafique A, Mahmood Zia K, Zuber M, Tabasum S, Rehman S. Chitosan functionalized poly(vinyl alcohol) for prospects biomedical and industrial applications: A review. Int J Biol Macromol. 2016;87:141–54.

31. Bhagath S, Vivek A, Krishna VV, Mittal SS, Balachandran M. Synthesis and characteristics of MMT reinforced chitosan nanocomposite. Mater Today Proc. 2021;46:4487–92.

32. Meigoli Boushehrian M, Esmaeili H, Foroutan R. Ultrasonic assisted synthesis of Kaolin/CuFe2O4 nanocomposite for removing cationic dyes from aqueous media. J Environ Chem Eng. 2020;8(4):103869.

33. Belaroussi A, Labed F, Khenifi A, Akbour RA, Bouberka Z, Kameche M, et al. A novel approach for removing an industrial dye 4GL by an Algerian Bentonite. Acta Ecol Sin. 2018;38(2):148–56.

34. Carvalho LB, Chagas PMB, Pinto LMA. Caesalpinia ferrea Fruits as a Biosorbent for the Removal of Methylene Blue Dye from an Aqueous Medium. Water, Air, Soil Pollut. 2018;229(9):297.

35. Foroutan R, Mohammadi R, Razeghi J, Ramavandi B. Performance of algal activated carbon/Fe3O4 magnetic composite for cationic dyes removal from aqueous solutions. Algal Res. 2019;40:101509.

36. Absalan G, Bananejad A, Ghaemi M. Removal of Alizarin Red and Purpurin from Aqueous Solutions Using Fe3O4 Magnetic Nanoparticles. Anal Bioanal Chem Res. 2017;4(1):65–77.

37. Nair BP, Pavithran C, Sudha JD, Prasad VS. Microvesicles through Self-Assembly of Polystyrene−Clay Nanocomposite. Langmuir. 2010 Feb;26(3):1431–4.

38. Sinha Ray S, Okamoto M. Polymer/layered silicate nanocomposites: a review from preparation to processing. Prog Polym Sci. 2003;28(11):1539–641.

39. Vaia RA, Vasudevan S, Krawiec W, Scanlon LG, Giannelis EP. New polymer electrolyte nanocomposites: Melt intercalation of poly(ethylene oxide) in mica-type silicates. Adv Mater. 1995 Feb;7(2):154–6.

40. Helal E, Amurin LG, Carastan DJ, de Sousa RR, David E, Fréchette M, et al. Interfacial molecular dynamics of styrenic block copolymer-based nanocomposites with controlled spatial distribution. Polymer (Guildf). 2017;113:9–26.

41. Vaia RA, Ishii H, Giannelis EP. Synthesis and properties of two-dimensional nanostructures by direct intercalation of polymer melts in layered silicates. Chem Mater. 1993 Dec;5(12):1694–6.

42. Romero-Fierro D, Bustamante-Torres M, Bravo-Plascencia F, Magaña H, Bucio E. Polymer-Magnetic Semiconductor Nanocomposites for Industrial Electronic Applications. Polymers (Basel). 2022;14(12):1–23.

43. Alexandre M, Dubois P. Polymer-layered silicate nanocomposites:

preparation, properties and uses of a new class of materials. Mater Sci Eng R Reports. 2000;28(1):1–63.

44. Ramakoti IS, Panda AK, Gouda N. A brief review on polymer nanocomposites: current trends and prospects. 2023;43(8):651–79.

45. Ganguly S, Dana K, Mukhopadhyay TK, Parya TK, Ghatak S. Organophilic Nano Clay: A Comprehensive Review. Trans Indian Ceram Soc. 2011 Oct;70(4):189–206.

46. Mascarenhas R, Kaur G. Electrically conductive polymer - Clay nanocomposites. AIP Conf Proc. 2023 May;2535(1):60010.

47. Nabirqudri SAM, Roy AS, Ambika Prasad MVN. Electrical and mechanical properties of free-standing PMMA–MMT clay composites. J Mater Res. 2014/11/12. 2014;29(24):2957–64.

48. Loganathan S, Pugazhenthi G, Thomas S, Varghese TO. An Overview of Polymer-Clay Nanocomposites. Clay-Polymer Nanocomposites. 2017;29–81.

49. Mehendru PC, Kumar N, Arora VP, Gupta NP. Dielectric relaxation studies in polyvinyl butyral. J Chem Phys. 1982 Oct;77(8):4232–5.

50. Babel S, Kurniawan TA. Low-cost adsorbents for heavy metals uptake from contaminated water: a review. J Hazard Mater. 2003;97(1):219–43.

51. ca293db4748d2714af1e46c4c3ceb789.pdf.

52. Ruiz GAM, Corrales HFZ. Chitosan, chitosan derivatives and their biomedical applications. Biol Act Appl Mar polysaccharides. 2017;87.

53. Peña-Parás L, Sánchez-Fernández JA, Vidaltamayo R. Nanoclays for Biomedical Applications BT - Handbook of Ecomaterials. In: Martínez LMT, Kharissova OV, Kharisov BI, editors. Cham:

Springer International Publishing; 2017. p. 1–19.

54. Nic M, Hovorka L, Jirat J, Kosata B, Znamenacek J. IUPAC compendium of chemical terminology-the gold book. International Union of Pure and Applied Chemistry; 2005.

55. Page C, Püntener A. European Ban on Certain Dyes. Tfl. 2012;5.

56. Hunger K, Mischke P, Rieper W, Raue R, Kunde K, Engel A. Azo Dyes. In: Ullmann's Encyclopedia of Industrial Chemistry. 2000.

57. Yuzhen Zhang, Wenfu Hou, Yueping Tan. Structure and dyeing properties of some anthraquinone violet acid dyes. Dye Pigment. 1997;34(1):25–35.

58. Venkataraman K. The Chemistry of Synthetic Dyes V4. Vol. 4. Elsevier; 2012.

59. Hallas G, Towns AD. Dyes derived from aminothiophenes. Part 7: Synthesis and properties of some benzo[b]thiophene-based azo disperse dyes. Dye Pigment. 1997;35(3):219–37.

60. Derkowska-Zielinska B, Skowronski L, Biitseva A, Grabowski A, Naparty MK, Smokal V, et al. Optical characterization of heterocyclic azo dyes containing polymers thin films. Appl Surf Sci. 2017;421:361–6.

61. Kapdan IK, Kargi F. Simultaneous biodegradation and adsorption of textile dyestuff in an activated sludge unit. Process Biochem. 2002;37(9):973–81.

62. Crini G. Non-conventional low-cost adsorbents for dye removal: A review. Bioresour Technol. 2006;97(9):1061–85.

63. Reish MS. Asian textile dye makers are a growing power in a changing market. Chem Eng News. 1996;15:10–2.

64. Doulati Ardejani F, Badii K, Yousefi Limaee N, Mahmoodi NM, Arami M, Shafaei SZ, et al. Numerical modelling and laboratory

studies on the removal of Direct Red 23 and Direct Red 80 dyes from textile effluents using orange peel, a low-cost adsorbent. Dye Pigment. 2007;73(2):178–85.

65.   Ho YS, Chiang CC. Sorption Studies of Acid Dye by Mixed Sorbents. Adsorption. 2001;7(2):139–47.

66.   Xing G, Liu S, xu Q, Liu Q. Preparation and adsorption behavior for brilliant blue X-BR of the cost-effective cationic starch intercalated clay composite matrix. Carbohydr Polym. 2012;87(2):1447–52.

67.   Raju A, Lakshmi V, Vishnu Prataap RK, Resmi VG, Rajan TPD, Pavithran C, et al. Adduct modified nano-clay mineral dispersed polystyrene nanocomposites as advanced corrosion resistance coatings for aluminum alloys. Appl Clay Sci [Internet]. 2016;126:81–8. Available from: https://www.sciencedirect.com/science/article/pii/S0169131716301053

68.   Di Y, Iannace S, Di Maio E, Nicolais L. Nanocomposites by melt intercalation based on polycaprolactone and organoclay. J Polym Sci Part B Polym Phys [Internet]. 2003 Apr 1;41(7):670–8. Available from: https://doi.org/10.1002/polb.10420

69.   Schlemmer D, Angélica RS, Sales MJA. Morphological and thermomechanical characterization of thermoplastic starch/montmorillonite nanocomposites. Compos Struct [Internet]. 2010;92(9):2066–70. Available from: https://www.sciencedirect.com/science/article/pii/S0263822309004590

70.   Vercelheze AES, Oliveira ALM, Rezende MI, Muller CMO, Yamashita F, Mali S. Physical Properties, Photo- and Bio-

degradation of Baked Foams Based on Cassava Starch, Sugarcane Bagasse Fibers and Montmorillonite. J Polym Environ [Internet]. 2013;21(1):266–74. Available from: https://doi.org/10.1007/s10924-012-0455-0

71. Aouada FA, Mattoso LHC, Longo E. New strategies in the preparation of exfoliated thermoplastic starch–montmorillonite nanocomposites. Ind Crops Prod [Internet]. 2011;34(3):1502–8. Availablefrom:https://www.sciencedirect.com/science/article/pii/S0 926669011001373